JOURNAL OF AGRICULTURAL AND FOOD CHEMISTRY

Food and Beverage Chemistry/Biochemistry

Flazin as a promising Nrf2 pathway activator

Hirotoshi Fuda, Satoshi Miyanaga, Takayuki Furukawa, Satomi Umetsu, Sae Joko, Yuning Roan, Hirotaka Suzuki, Shu-Ping Hui, Mitsugu Watanabe, and Hitoshi Chiba

J. Agric. Food Chem., **Just Accepted Manuscript** • DOI: 10.1021/acs.jafc.9b04600 • Publication Date (Web): 31 Oct 2019

is published by the American Chemical Society. 1155 Sixteenth Street N.W., Washington, DC 20036

Title: Flazin as a promising Nrf2 pathway activator

Authors: Hirotoshi Fuda [a, 1], Satoshi Miyanaga [a, 1], Takayuki Furukawa [a, 1], Satomi Umetsu [a], Sae Joko [a], Yuning Roan [a], Hirotaka Suzuki [a], Shu-Ping Hui [a *], Mitsugu Watanabe [b], and Hitoshi Chiba [c]

Affiliations: [a] Faculty of Health Sciences, Hokkaido University, Sapporo 060-0812, Japan; [b] Watanabe Oyster Laboratory Co. Ltd., 490-3, Shimoongata-cho, Hachioji, Tokyo 190-0154, Japan; [c] Department of Nutrition, Sapporo University of Health Sciences, Nakanuma Nishi-4-2-1-15, Higashi-ku, Sapporo 007-0894, Japan

[1] These authors contributed equally to this work.

*** Corresponding author:** Shu-Ping Hui

Address: Faculty of Health Sciences, Hokkaido University, Kita-12, Nishi-5, Kita-ku, Sapporo 060-0812, Japan,

+81.11.706.3693, Email: keino@hs.hokudai.ac.jp

ABSTRACT

Flazin is a β-carboline-derived alkaloid found in Japanese fermented foods. Here, the potential of flazin as an antioxidant food was studied with particular reference to its effect on the Keap1-Nrf2 system in human hepatocytes (C3A). Flazin, flazin analogues including the decarboxylated derivative perlolyrine were chemically synthesized and compared with each other and with chlorogenic acid and curcumin. Among these compounds, flazin showed the lowest cytotoxicity (IC_{50}<500 μM) and the highest capacity to activate Keap1-Nrf2 system. It provided the largest (>3-fold of control) cytoprotection ability against a pro-oxidant, although its radical absorbance capacity was relatively low. Flazin increased the expressions of Nrf2-dependent phase II enzyme genes, and their products (NQO1, GSTP and GSH proteins). The strong cytoprotection ability of flazin associated with low log*P* (0 to 3) is shared by sulforaphane and 3,5-dihydroxy-4-methoxybenzyl alcohol, suggesting potential value of flazin and flazin-rich foods for prevention of oxidation-related health disorders.

Keywords: Keap1; Nrf2; hepatocyte; phase II enzyme; flazin; ORAC

1. INTRODUCTION

The balance of reactive oxygen species (ROS) is maintained by a cytoprotection system whose components can be divided into enzymatic components (superoxide dismutase [SOD], catalase [CAT], etc.) and non-enzymatic components (glutathione [GSH], vitamins, etc.) [1]. Non-compensated overproduction of ROS damages cells, causing ageing [2] and various pathological conditions, such as neoplasia [3], inflammation [4], atherosclerosis [5], and neurodegenerative diseases [6]. Ingestion of phenolic antioxidants in foods is crucially important for health and for the maintenance of physiological conditions resistant to ROS [7].

Dinkova-Kostova and Talalay proposed classifying antioxidants into two groups: direct and indirect antioxidants [8]. Direct antioxidants scavenge ROS through redox reactions. During this process, the direct antioxidants are chemically oxidized and in some cases regenerated [9,10]. The antioxidant potential of direct antioxidants can be evaluated through *in vitro* chemical analyses, such as 2,2-diphenyl-1-picrylhydrazyl (DPPH) assays or oxygen radical absorbance capacity (ORAC) assays. On the other hand, indirect antioxidants induce a series of antioxidant enzymes or low-molecular-weight substances by activating the Kelch-like ECH-associated protein 1 (Keap1)-nuclear factor erythroid 2-related factor 2 (Nrf2) pathway and thus ultimately

biologically catalyse ROS breakdown in cells. Indirect antioxidants may be redox active, but this characteristic is not necessary for their indirect antioxidant activity [8].

The role of the Keap1-Nrf2 pathway to pathological conditions has been studied in human patients and Nrf2-deficient and/or Keap1-deficient mice. These studies reported that Nrf2 activation alleviated (or exacerbated) the pathological conditions including neurodevelopmental disorder, chronic kidney disease, neurodegenerative disorders, pulmonary hypertension, emphysema and cancer [11,12]. In human patients, the Nrf2-activators, sulforaphane and bardoxolone methyl (CDDO-Me), alleviated the symptom of the neurodevelopmental disorder [13] and chronic kidney disease [14], respectively. Using both Nrf2-deficient and Keap1-deficient mice, oltipraz (Nrf2 activator) attenuated pulmonary hypertension [15]. In Nrf2-deficient mice, smoking increased inflammation in the lung and induced emphysema [16]. In cancer, Nrf2 activation was beneficial or deleterious for cancer-bearing host depending on the time and the place of body [11]. Using Nrf2-deficient mice, Nrf2 activator of oltipraz reduced the number of neoplasms of the forestomach [17]. However, activation of Nrf2 mediated by dipeptidyl peptidase-4 inhibitors (Sax and Sit) enhanced tumor metastasis [18].

Flazin is a β-carboline-derived alkaloid found in Japanese fermented foods such as Japanese rice wine lees, rice vinegar, soy sauce, and soy paste [19]; it has also been

found in a marine bacterium [20] and in a fungus from China [21]. Flazin has been reported to induce NAD(P)H: quinone oxidoreductase (NQO1) in a murine hepatoma cell line [22]. Since NQO1 belongs to the family of Nrf2-dependent phase II antioxidant enzymes, we aimed to uncover the possible relationship of flazin and its analogues with the Keap1-Nrf2 pathway in this study.

To this end, we chemically synthesized flazin, four analogues [21] and decarboxylated derivertive perlolyrine in the present study. Furthermore, we compared these compounds with chlorogenic acid and curcumin, which are representative direct and indirect antioxidants, respectively [23], in assessments of cytotoxicity, ORAC, Keap1-Nrf2 pathway activation, and cytoprotection against oxidative stress.

In addition, we here propose a model for predicting the usefulness of antioxidants in which log *P* and cytoprotective effects against oxidative stress serve as determinant factors. Log *P*, or the partition coefficient [24], is common in drug design in the pharmaceutical and biotechnology industries as a measure of a solute's hydrophobicity and as a proxy for its membrane permeability; however, this parameter has been uncommon in the food industry. Our proposed model reveals a unique position of flazin among antioxidants, indicating its remarkable potential with regard to the prevention and/or alleviation of health disorders involving oxidation processes.

2. MATERIALS AND METHODS

2.1. Chemicals. The chemicals used in this study were described in the Supporting Materials and Methods.

2.2. n-Octanol/water partition coefficients (log *P* values). The n-octanol/water partition coefficients (log P_{ow} or log *P* values) of flazin and perlolyrine were obtained from the PubChem Open Chemistry Database (*https://pubchem.ncbi.nlm.nih.gov/search/*) maintained by the National Institutes of Health (NIH). The log *P* values for the flazin analogues, chlorogenic acid (**8**), and curcumin (**7**) were obtained from the Virtual Computational Chemistry Laboratory (*http://www.vcclab.org/lab/alogps/*) and the literature [25-26].

2.3. Chemical synthesis

2.3.1. General. The chemicals and procedures in chemical synthesis were described in the Supporting Materials and Methods.

2.3.2. Synthesis of flazin and its analogues. The structures of the compounds synthesized in this study as well as those of chlorogenic acid (**8**) and curcumin (**7**) are shown in Fig. 1. Flazin (**1**) and its analogues (**3**-**6**) were synthesized as reported by Tang *et al*. [21], and each synthesized compound was confirmed to be identical to the

previous report on the basis of NMR chemical shifts and the molecular weights determined by mass spectrometry.

2.3.3. Synthesis of perlolyrine

2.3.3.1. Synthesis of compound 10. The synthesis of compound **10** and data of proton and carbon NMR were described in the Supporting Materials and Methods.

2.3.3.2. Synthesis of compound 11. The synthesis of compound **11** and data of proton and carbon NMR were described in the Supporting Materials and Methods.

2.3.3.3. Synthesis of perlolyrine (2). The synthesis of perlolyrine **(2)** and data of proton and carbon NMR were described in the Supporting Materials and Methods.

2.4. Cell culture. Human hepatoma-derived cells (C3A) were purchased from the ATCC. The cells were maintained in MEM supplemented with 10% (v/v) FBS and the PSN antibiotic mixture under an atmosphere of 5% CO_2 and 95% air in an incubator with controlled humidity at 37°C.

2.5. Cytotoxicity assay. All procedures were performed according to a previously described protocol, with minor modifications [27]. Cytotoxicity assay in details was performed as indicated in the Supporting Materials and Methods.

2.6. Reporter gene assay. Reporter gene assay in details was performed as indicated in the Supporting Materials and Methods. Chlorogenic acid (**8**) and curcumin (**7**) were

used as negative and positive controls, respectively, in the reporter gene assay since we previously reported that curcumin significantly increases relative luciferase activity, while chlorogenic acid does not significantly affect it [23].

2.7. Cytoprotection assay. Cytoprotection assay in details was performed as indicated in the Supporting Materials and Methods.

2.8. First-strand cDNA synthesis and real-time PCR. Total RNA extracts, first-strand cDNA synthesis and real-time PCR were performed as indicated in the Supporting Materials and Methods.

2.9. Western blot analysis. Protein expression induced by flazin (**1**) in C3A cells was examined using Western blotting. All procedures were performed according to a previously described protocol, with minor modifications [23]. Western blot analysis in details was performed as indicated in the Supporting Materials and Methods.

2.10. Nuclear protein extraction and Western blot analysis. The effect of flazin (**1**) on the translocation of the Nrf2 protein from the cytoplasm to the nucleus was examined using nuclear protein extraction and Western blotting. Nuclear protein extraction and Western blot analysis in details was performed as indicated in the Supporting Materials and Methods.

2.11. Measurement of glutathione (GSH). The effect of flazin (**1**) on GSH levels in

C3A cells was examined. All procedures were performed according to a previously described protocol, with minor modifications [23]. Measurement of glutathione in details was performed as indicated in the Supporting Materials and Methods.

2.12. Oxygen radical absorbance capacity (ORAC) assay. The free radical-scavenging activity of the antioxidants was examined using ORAC assays. All procedures were performed according to a previously described protocol [28-29]. The relative ORAC value (TE) was calculated as follows: relative ORAC value = molarity of Trolox/molarity of the samples.

2.13. Statistical analysis. The data from the reporter gene assay, cell viability assay, and ORAC assay and the data from the nuclear protein, Nrf2 target gene and protein expression analyses are expressed as the mean ± SD and were analysed by one-way ANOVA using Prism 6.03. The significance level was set at $p < 0.05$.

3. RESULTS

3.1. Cytotoxicity. The half-maximal inhibitory concentration (IC_{50}) values for synthetic flazin (**1**), perlolyrine (**2**) and the flazin analogues are shown in Supplemental Fig. 1 and Table 1. The IC_{50} values of flazin (**1**) and chlorogenic acid (**8**) were more than 500 μM. In contrast, those of perlolyrine (**2**), curcumin (**7**), flazin analogue Ⅰ (**3**), flazin analogue

II (**4**), flazin analogue III (**5**), and flazin analogue IV (**6**) were low at 11.0, 109, 51.5, 88.2, 12.0, and 22.4 μM, respectively.

3.2. ORAC assay. The relative ORAC values of the antioxidants are shown in Table 1. The relative ORAC values of flazin (**1**), perlolyrine (**2**), flazin analogue II (**4**), and flazin analogue III (**5**) were 1.43 ± 0.112, 1.60 ± 0.230, 0.587 ± 0.124, and 0.886 ± 0.0735 μmol of Trolox equivalents (TE)/μmol, respectively. In contrast, those of flazin analogue I (**3**) and flazin analogue IV (**6**) were relatively high (3.65 ± 0.392 and 2.50 ± 0.287 μmol of TE/μmol, respectively). Curcumin (**7**) and secondarily chlorogenic acid (**8**) showed the highest ORAC values: 8.12 ± 0.831 and 4.57 ± 0.303 μmol of TE/μmol, respectively.

3.3. Reporter gene assay. The results of the reporter gene assay for the studied compounds at non-cytotoxic concentrations are shown in Fig. 3A and Table 1. Compared to the control treatment (0 μM), flazin (**1**) treatment at concentrations of 0-500 μM dose-dependently increased relative luciferase activity by 23.4 ± 0.861-fold; these effects were comparable to those of curcumin (**7**)(23.8 ± 7.30-fold increase at concentrations of 20-40 μM). Perlolyrine (**2**) increased relative luciferase activity by 4.64 ± 0.812-fold at concentrations of 4-8 μM. Flazin analogue II (**4**) at concentrations of 10-20 μM increased the luciferase activity by 10.50 ± 4.5-fold. However, chlorogenic acid (**8**), flazin analogue I (**3**), flazin analogue III (**5**), and flazin analogue IV (**6**) did not

significantly affect the relative luciferase activity at any concentration.

3.4. Cytoprotection against pro-oxidants. The effects of the studied compounds at non-cytotoxic concentrations on the viability of C3A cells exposed to the pro-oxidant (AAPH) are shown in Fig. 3B and Table 1. Flazin (**1**) significantly and dose-dependently increased cell viability by 5.21 ± 0.24-fold at concentrations of 0-500 μM. Curcumin (**7**) also significantly and dose-dependently increased viability by 2.66 ± 0.253-fold at concentrations of 15-60 μM, and flazin analogue II (**4**) increased viability by 2.00 ± 0.176-fold at concentrations of 10-20 μM. Perlolyrine (**2**), chlorogenic acid (**8**), flazin analogue I (**3**), flazin analogue III (**5**), and flazin analogue IV (**6**) did not significantly affect cell viability at any concentration.

3.5. Effect of flazin on Nrf2 nuclear translocation and the expression of Nrf2 and Keap1. The effect of flazin (**1**) on Nrf2 nuclear translocation in C3A cells is shown in Fig. 4A and 4B. Compared to the control treatment (0 μM), flazin (**1**) treatment at concentrations of 0-500 μM significantly and dose-dependently increased the protein levels of Nrf2 in the nucleus fraction by approximately 1.5-fold. And flazin decreased the levels of Nrf2 in the cytoplasmic fraction at concentrations of 250-500 μM by approximately one-half. Also flazin increased the protein and gene expression in total lysates Nrf2 levels in a dose-dependent manner (Fig. 4C and D). Flazin decreased the

protein expression of Keap1 levels at 500 μM (Fig. 4E).

3.6. Effect of flazin on the expression of Nrf2 target genes. The Nrf2 target genes induced by flazin in C3A cells are shown in Fig. 5A. Flazin (**1**) significantly induced the expression of the Nrf2 target genes *NQO1*, glutamate-cysteine ligase modulatory subunit (*GCLM*), glutamate-cysteine ligase catalytic subunit (*GCLC*) and glutathione S-transferase pi (*GSTP*) by more than 10-fold in a dose-dependent manner. More moderate but statistically significant induction was observed for *HO-1*, *SOD1*, *GR*, *GPx*, *CAT*, and *GSTT*.

3.7. Effect of flazin on the expression of Nrf2 target gene products. We paid attention to the Nrf2 target genes, *NQO1*, *GSTP*, *GCLM* and *GCLC* whether they were induced by flazin significantly (more than 10-fold) and the change in their protein expressions. The effects of flazin (**1**) on the expression of three Nrf2 target gene products, NQO1, GSTP and GSH, which is synthesized by composed of GCLC and GCLM, are shown in Fig. 5B. Flazin (**1**) increased the protein expression of NQO1 and GSH in a dose-dependent manner. In addition, flazin (**1**) significantly increased GSTP expression levels at 500 μM.

3.8. Cytoprotection and log *P*. The log *P* values of the studied compounds are shown in Table 1. The highest log *P* was observed for curcumin (3.29), while the lowest was

observed for chlorogenic acid (0.69). The log *P* values of flazin (2.1), perlolyrine (2.2), and the flazin analogues (1.72-2.80) were in the middle range. For eight of the natural antioxidants (a - h), there was a strong correlation between cytoprotection and the log *P* value ($y = 0.400x + 0.880$, $r^2 = 0.766$, $p = 0.004$) (Fig. 7). For another group of four natural antioxidants (f - i), there was also a strong correlation between cytoprotection and the log *P* value ($y = 0.059x + 1.974$, $r^2 = 0.750$, $p = 0.333$) (Fig. 7). The antioxidants flazin, 3,5-dihydroxy-4-methoxybenzyl alcohol (DHMBA) and sulforaphane did not fit the correlation lines and were distributed in division Ⅰ.

4. DISCUSSION

Flazin has been reported to be present in traditional Japanese fermented foods, such as sake (rice wine) lees, rice vinegar, soy sauce (fermented soybean liquid), and miso (fermented soybean paste) [19], as well as in the fruiting bodies of *Suillus granulatus* (a fungus) [21] and in the marine-derived bacteria *Streptomyces* spp. [20]. With regard to biological function, flazin exhibits anti-HIV-1 activity [21], NQO1-inducing activity [22], leukaemic cell (HL-60) proliferation-inhibiting activity [30], and xanthine oxidase-inhibiting activity [31]. In our present study, flazin was found to activate the Nrf2 pathway (Fig. 3A and 4A) and to promote the expression of a battery of Nrf2 target genes and products,

including NQO1 (Fig. 5A and B). Flazin exhibit a strong cytoprotective effect against AAPH despite its relatively low ORAC, suggesting that flazin essentially serves as an indirect antioxidant. The action mechanisms of flazin as an indirect antioxidant are summarized in Fig. 6.

The relationships between the chemical structures and anti-HIV activity of flazin and its 45 synthetic analogues have been reported previously [21]. In this study, the highest anti-HIV activity was observed for flazin analogue III (**5**), in which the carboxylic acid at carbon 3 of flazin has been converted to an amide [21] (Fig. 1). Flazin itself was found not to exhibit anti-HIV-1 activity; thus, the activity was dramatically enhanced by the introduction of an appropriate substituent at carbon 3. In contrast to anti-HIV-1 activity, indirect antioxidant activity requires the carboxylic at position 3. Naturally occurring flazin showed higher cytotoxicity, stronger Nrf2-activating ability, and greater cytoprotective effects than the flazin analogues or perlolyrine (Supplemental Fig. 1, Fig. 3 and Table 1). Conversely, flazin analogue III (**5**) showed the lowest performance in cytoprotection.

The ORAC assay is one of the most common assays for measuring peroxyl radical-scavenging capacity *in vitro*, although its reaction mechanism remains unknown [32]. In this study, the ORAC values of flazin analogues I (**3**) and IV (**6**) (3.65 ± 0.392 and

2.50 ± 0.287 μmol of TE/μmol, respectively) were higher than that of flazin (**1**) (1.43 ± 0.112 μmol of TE/μmol) (Table 1). In flazin analogues Ⅰ (**3**) and Ⅳ (**6**), the carboxylic acid at carbon 3 of flazin has been replaced with a hydroxamic acid and aliphatic alcohol, respectively (Fig. 1). We hypothesize that the hydroxamic acid and aliphatic alcohol of the flazin analogues might easily form R-C(O)-NH-O● and R-C-O●, respectively, to enable these analogues to scavenge peroxyl radicals in the ORAC assay more easily than flazin.

When exposed to oxidative stress or Nrf2 activators, several highly reactive cysteine residues of Keap1 are modified to prevent Nrf2 from proteasome degradation, resulting in rapid nuclear translocation of Nrf2 [11]. Resveratrol-treated HaCat cells (spontaneously immortalized human keratinocytes) have been investigated on the Nrf2 and Keap1 levels in total cell lysates, and on the Nrf2 levels in nuclear and cytoplasmic fractions [33]. Resveratrol increased the Nrf2 levels in the nuclear fraction, but decreased them in the cytoplasmic fraction. These results are in agreement with the present study (Fig. 4A and 4B), where flazin-induced nuclear translocation of Nrf2 was confirmed. In flazin-treated C3A cells, upregulation of Nrf2 levels and downregulation of Keap1 levels in the total cell lysate were indicated (Fig. 4C-E). Flazin might have stabilized Nrf2 protein in the cytosol and accelerated its nuclear translocation. Similarly, resveratrol has

been reported to increase Nrf2 levels in the total cell lysate with significant reduction in the levels of Keap1 [33].

The potent cytoprotective effect of flazin can be attributed at least partly to the induction of a battery of antioxidant enzymes by flazin through activation of the Nrf2 pathway. Flazin induced the expression of Nrf2 protein and of the Nrf2 target genes *HO-1*, *GCLM*, *GCLC*, *NQO1*, *SOD1*, *GR*, *GPx*, and *GSTP* (Fig. 5A and 5B). Of these, *NQO1*, *GCLM*, *GCLC*, and *GSTP* and their products showed substantially increased expression (Fig. 5A and 5B). The catalytic activity of NQO1 is directed towards the reduction and detoxication of highly reactive quinones and their derivatives. NQO1 is expressed in many tissues, and its expression is co-regulated by the Keap1-Nrf2 pathway [34]. GSTP is a type of cytosolic GST and plays an important role in the classic GSH-dependent enzymatic detoxification pathway of electrophilic metabolites and xenobiotics [35]. Nrf2 is one of the most important transcription factors recognized to stimulate GSTP [36]. GSH is present at micromolar levels in all eukaryotic cells and provides protection against ROS [37]. GSH is synthesized by glutamate-cysteine ligase (GCL), which is composed of GCLC and GCLM, and GSH synthetase. GCL catalyses the rate-limiting step in GSH synthesis and is the site of feedback inhibition by GSH itself [38]. Both human GCLC and GCLM are regulated by the Keap1-Nrf2 pathway [37]. In

this study, the increased expression of *GCLC* and *GCLM* due to flazin-induced Nrf2 activation was associated with an increase in GSH (Fig. 5C). The increase in GSH, however, might be too small (2.6-fold) to fully account for the observed increases in *GCLM* and *GCLC* expression of 12.7- and 42.5-fold, respectively. We propose that synthesized GSH inhibits the catalytic activity of GCL.

In our previous study, we examined log *P* in ten natural antioxidants [23]. In a scatter plot showing the cytoprotective effect plotted against the log *P* for each antioxidant, most antioxidants were distributed along a single curve. However, sulforaphane and DHMBA showed unique distributions. A new scatter plot including the present data is shown in Fig. 7, in which 4 divisions (I-IV) have been made on the basis of cytoprotection (dividing line at 3-fold greater than control values) and log *P* (dividing line at 3). Flazin is distributed in division I (upper left) together with sulforaphane and DHMBA; moreover, flazin occupies the highest position among them in terms of its cytoprotection. In contrast to flazin, the flazin analogues, perlolyrine and other antioxidants are distributed along a curve in division III. With regard to sulforaphane and DHMBA, studies have reported their usefulness in preventing and/or alleviating health disorders; for instance, anticancer, anti-diabetes, and anti-inflammatory effects have been reported for sulforaphane [39-40], and anti-non-alcoholic steatohepatitis (NASH)

effects have been reported for DHMBA [41]. On the basis of the above evidence, flazin and flazin-rich foods may also have a promising future as functional foods.

As shown in the scatter plot, log *P* appears to increase the cytoprotective ability of the antioxidants in division III (Fig. 7). However, the effect of log *P* reaches a plateau in division IV. This can be explained by the association of higher log *P* values with higher cytotoxicity (Table 1). It is a general rule that hydrophobic compounds (with higher log *P* values) are more toxic in the body than hydrophilic compounds (with lower log *P* values) [24]. Flazin and perlolyrine (e in Fig. 7) exhibited large differences in cytoprotection despite their similar log *P* values, indicating that log *P* is not the only determinant of cytoprotective ability. This difference must be due to the Nrf2-activating ability of flazin, since divisions I and III are clearly separated at the cytoprotection level of approximately 3-fold (Fig. 7). Since only a few antioxidants (sulforaphane, j; DHMBA, k; and flazin) have been specified as belonging to division I so far, further surveys of novel indirect antioxidants belonging to division I are warranted.

This study indicates that flazin is a potentially useful functional food for antioxidants *via* activating Keap1-Nrf2 pathway. However, possible adverse effect of flazin remains to be investigated. Flazin belongs to β-carboline derivatives, which is supposed to generate through the Maillard reaction as previously reported [42,43]. The Maillard reaction

products have both positive and negative effects on health such as antioxidants, bacterucidals, antiallegenic, prooxidant, and carcinogens [44-47]. The utility of flazin as a functional food needs to be examined by animal model experiments and human trials in future.

5. CONCLUSION

Flazin activates the Nrf2 pathway and protects human hepatocytes from oxidative stress without showing any significant cytotoxicity. The potential for flazin to be used as a functional food must be investigated in future animal model experiments and subsequent human trials. Since log *P* values are accessible in chemical databases and are useful for predicting the utility of individual antioxidants, a log *P*-based search for indirect antioxidant foods is recommended. The limitation of this study is the lack of *in vivo* confirmation of the effect and the safety of flazin. These issues remain to be studied in the future.

COMPETING INTERESTS.

This study was partially funded by Watanabe Oyster Laboratory Co. Ltd., and Hirotoshi Fuda works in a research laboratory donated by them. The funder had no role

in the study design, data collection and analysis, decision to publish, or preparation of the manuscript.

ACKNOWLEGEMENTS.

The anti-Nrf2 antibodies were kindly donated by Dr. Masaharu Sakai, professor emeritus, Hokkaido University. This work was financially supported by a Grant-in-Aid for Scientific Research from the JSPS (16K07863), by the Regional Innovation Strategy Support Program of the MEXT and by Watanabe Oyster Laboratory Co. Ltd. The English proofreading by Dr. Darwish W. S. was very useful.

ABBREVIATIONS.

AAPH, 2,2'-azobis(2-amidinopropane) dihydrochloride; **DHMBA**, 3,5-dihydroxy-4-methoxybenzyl alcohol; **ORAC**, oxygen radical absorbance capacity.

REFERENCES

(1) Wiernsperger, N. F. Oxidative stress as a therapeutic target in diabetes: revisiting the controversy. *Diabetes Metab.* **2003**, *29*, 579-585.

(2) Kauppila, T. E. S.; Kauppila, J. H. K.; Larsson, N. G. Mammalian mitochondria and aging: An Update. *Cell Metab.* **2017**, *25*, 57-71.

(3) Prasad, S.; Gupta, S. C.; Tyagi, A. K. Reactive oxygen species (ROS) and cancer: Role of antioxidative nutraceuticals. *Cancer Lett.* **2017**, *387*, 95-105.

(4) Blaser, H.; Dostert, C.; Mak, T. W.; Brenner, D. TNF and ROS Crosstalk in Inflammation. *Trends Cell Biol.* **2016**, *26*, 249-261.

(5) Forstermann, U.; Xia, N.; Li, H. Roles of vascular oxidative stress and nitric oxide in the pathogenesis of Atherosclerosis. *Circ. Res.* **2017**, *120*, 713-735.

(6) Tonnies, E.; Trushina, E. Oxidative stress, synaptic dysfunction, and Alzheimer's disease. *J. Alzheimer's Dis.* **2017**, *57*, 1105-1121.

(7) Shahidi, F.; Ambigaipalan, P. Phenolics and polyphenolics in foods, beverages and spices: Antioxidant activity and health effects - A review. *J. Funct. Foods* **2015**, *18*, 820-897.

(8) Dinkova-Kostova, A. T.; Talalay, P. Direct and indirect antioxidant properties of

inducers of cytoprotective proteins. *Mol. Nutr. Food Res.* **2008**, *52*, S128-38.

(9) Villuendas-Rey, Y.; Alvarez-Idaboy, J. R.; Galano, A. Assessing the protective activity of a recently discovered phenolic compound against oxidative stress using computational chemistry. *J. Chem. Inf. Model.* **2015**, *55*, 2552-2561.

(10) Pedrielli, P.; Skibsted, L. H. Antioxidant synergy and regeneration effect of quercetin, (-)-epicatechin, and (+)-catechin on alpha-tocopherol in homogeneous solutions of peroxidating methyl linoleate. *J. Agr. Food Chem.* **2002**, *50*, 7138-7144.

(11) Yamamoto, M.; Kensler, T. W.; Motohashi, H. The KEAP1-NRF2 system: a thiol-based sensor-effector apparatus for maintaining redox homeostasis. *Physiol. Rev.* **2018**, *98*, 1169-1203.

(12) Hashimoto, K. Essential role of Keap1-Nrf2 signaling in mood disorders: overview and future perspective. *Front. Pharmacol.* **2018**, *9*, 1182.

(13) Lynch, R.; Diggins, E. L.; Connors, S. L.; Zimmerman, A. W.; Singh, K.; Liu, H.; Talalay, P.; Fahey, J. W. Sulforaphane from broccoli reduces symptoms of sutism: a follow-up case series from a randomized double-blind study. *Glob. Adv. Health Med.* **2017**, *6*, 2164957X17735826.

(14) de Zeeuw, D.; Akizawa, T.; Audhya, P.; Bakris, G. L.; Chin, M.; Christ-Schmidt, H.; Goldsberry, A.; Houser, M.; Krauth, M.; Lambers Heerspink, H. J.; McMurray, J. J.;

Meyer, C. J.; Parving, H. H.; Remuzzi, G.; Toto, R. D.; Vaziri, N. D.; Wanner, C.; Wittes, J.; Wrolstad, D.; Chertow, G. M. Bardoxolone methyl in type 2 diabetes and stage 4 chronic kidney disease. *N. Engl. J. Med.* **2013**, *369*, 2492-2503.

(15) Eba, S.; Hoshikawa, Y.; Moriguchi, T.; Mitsuishi, Y.; Satoh, H.; Ishida, K.; Watanabe, T.; Shimizu, T.; Shimokawa, H.; Okada, Y.; Yamamoto, M.; Kondo, T. The nuclear factor erythroid 2-related factor 2 activator oltipraz attenuates chronic hypoxia-induced cardiopulmonary alterations in mice. *Am. J. Respir. Cell Mol. Biol.* **2013**, *49*, 324-333.

(16) Rangasamy, T.; Cho, C. Y.; Thimmulappa, R. K.; Zhen, L.; Srisuma, S. S.; Kensler, T. W.; Yamamoto, M.; Petrache, I.; Tuder, R. M.; Biswal, S. Genetic ablation of Nrf2 enhances susceptibility to cigarette smoke-induced emphysema in mice. *J. Clin. Invest.* **2004**, *114*, 1248-1259.

(17) Ramos-Gomez, M.; Kwak, M. K.; Dolan, P. M.; Itoh, K.; Yamamoto, M.; Talalay, P.; Kensler, T. W. Sensitivity to carcinogenesis is increased and chemoprotective efficacy of enzyme inducers is lost in nrf2 transcription factor-deficient mice. *Proc. Natl. Acad. Sci .U S A* **2001**, *98*, 3410-3415.

(18) Wang, H.; Liu, X.; Long, M.; Huang, Y.; Zhang, L.; Zhang, R.; Zheng, Y.; Liao, X.; Wang, Y.; Liao, Q.; Li, W.; Tang, Z.; Tong, Q.; Wang, X.; Fang, F.; Rojo de la Vega,

M.; Ouyang, Q.; Zhang, D. D.; Yu, S.; Zheng, H. NRF2 activation by antioxidant antidiabetic agents accelerates tumor metastasis. *Sci. Transl. Med.* **2016**, *8*, 334ra51.

(19) Nakatsuka, S.; Feng, B.; Goto, T.; Kihara, K. Structures of flazin and YS, highly fluorescent compounds isolated from japanese soy sauce. *Tetrahedron Lett.* **1986**, *27*, 3399-3402.

(20) Shaaban, M.; Schröder, D.; Shaaban, K. A.; Helmke, E.; Grün-Wollny, I.; Wagner-Döbler, I.; Laatsch, H. Flazin, Perlolyrin, and other β-Carbolines from marine derived Bacteria. *Rev. Latinoam. Quím.* **2008**, *35*, 58-67.

(21) Tang, J. G.; Wang, Y. H.; Wang, R. R.; Dong, Z. J.; Yang, L. M.; Zheng, Y. T.; Liu, J. K. Synthesis of analogues of flazin, in particular, flazinamide, as promising anti-HIV agents. *Chem. Biodivers.* **2008**, *5*, 447-460.

(22) Li, Y.; Zhao, M.; Parkin, K. L. beta-carboline derivatives and diphenols from soy sauce are in vitro quinone reductase (QR) inducers. *J. Agr. Food Chem.* **2011**, *59*, 2332-2340.

(23) Joko, S.; Watanabe, M.; Fuda, H.; Takeda, S.; Furukawa, T.; Hui, S. P.; Shrestha, R.; Chiba, H. Comparison of chemical structures and cytoprotection abilities between direct and indirect antioxidants. *J. Funct. Foods* **2017**, *35*, 245-255.

(24) Leo, A.; Hansch, C.; Elkins, D. Partition coefficients and their uses. *Chem. Rev.*

1971, *71*, 525-616.

(25) Sergediene, E.; Jonsson, K.; Szymusiak, H.; Tyrakowska, B.; Rietjens, I. M.; Cenas, N. Prooxidant toxicity of polyphenolic antioxidants to HL-60 cells: description of quantitative structure-activity relationships. *FEBS Lett.* **1999**, *462*, 392-396.

(26) Ramalingam, P.; Yoo, S. W.; Ko, Y. T. Nanodelivery systems based on mucoadhesive polymer coated solid lipid nanoparticles to improve the oral intake of food curcumin. *Food Res. Int.* **2016**, *84*, 113-119.

(27) Fuda, H.; Watanabe, M.; Hui, S. P.; Joko, S.; Okabe, H.; Jin, S.; Takeda, S.; Miki, E.; Watanabe, T.; Chiba, H. Anti-apoptotic effects of novel phenolic antioxidant isolated from the Pacific oyster (*Crassostrea gigas*) on cultured human hepatocytes under oxidative stress. *Food Chem.* **2015**, *176*, 226-233.

(28) Watanabe, M.; Fuda, H.; Jin, S.; Sakurai, T.; Hui, S. P.; Takeda, S.; Watanabe, T.; Koike, T.; Chiba, H. A phenolic antioxidant from the Pacific oyster (*Crassostrea gigas*) inhibits oxidation of cultured human hepatocytes mediated by diphenyl-1-pyrenylphosphine. *Food Chem.* **2012**, *134*, 2086-2089.

(29) Watanabe, M.; Fuda, H.; Jin, S.; Sakurai, T.; Ohkawa, F.; Hui, S. P.; Takeda, S.; Watanabe, T.; Koike, T.; Chiba, H. Isolation and characterization of a phenolic antioxidant from the Pacific oyster (*Crassostrea gigas*). *J. Agr. Food Chem.* **2012**, *60*,

830-835.

(30) Nishio, M.; Yuasa, K.; Okimura, K.; Ogamo, M.; Imai, K.; Katsuzaki, H.; Matsunaga, M.; Umekawa, H. Cellular effects of Tamari soy sauce-derived 1-[5-(Hydroxymethyl)furan-2-yl]-9H-pyrido[3,4-b]indole-3-carboxylic acid (Flazin). *Food Sci. Technol. Res.* **2012**, *18*, 919-922.

(31) Li, H.; Zhao, M.; Su, G.; Lin, L.; Wang, Y. Effect of soy sauce on serum uric acid levels in hyperuricemic rats and identification of flazin as a potent xanthine oxidase inhibitor. *J. Agr. Food Chem.* **2016**, *64*, 4725-4734.

(32) Zhang, D.; Liu, Y. X.; Chu, L.; Wei, Y.; Wang, D.; Cai, S. B.; Zhou, F.; Ji, B. P. Relationship between the structures of flavonoids and oxygen radical absorbance capacity values: A quantum chemical analysis. *J. Phys. Chem. A* **2013**, *117*, 1784-1794.

(33) Liu, Y.; Chan, F.; Sun, H.; Yan, J.; Fan, D.; Zhao, D.; An, J.; Zhou, D. Resveratrol protects human keratinocytes HaCaT cells from UVA-induced oxidative stress damage by downregulating Keap1 expression. *Eur. J. Pharmacol.* **2011**, *650*, 130-137.

(34) Nioi, P.; Hayes, J. D. Contribution of NAD(P)H:quinone oxidoreductase 1 to protection against carcinogenesis, and regulation of its gene by the Nrf2 basic-region leucine zipper and the arylhydrocarbon receptor basic helix-loop-helix transcription

factors. *Mut. Res.* **2004**, *555*, 149-171.

(35) Bartolini, D.; Galli, F. The functional interactome of GSTP: A regulatory biomolecular network at the interface with the Nrf2 adaption response to oxidative stress. *J.Chrom. B* **2016**, *1019*, 29-44.

(36) Higgins, L. G.; Hayes, J. D. Mechanisms of induction of cytosolic and microsomal glutathione transferase (GST) genes by xenobiotics and pro-inflammatory agents. *Drug Metab. Rev.* **2011**, *43*, 92-137.

(37) Wild, A. C.;Mulcahy, R. T. Regulation of gamma-glutamylcysteine synthetase subunit gene expression: insights into transcriptional control of antioxidant defenses. *Free Radic. Res.* **2000**, *32*, 281-301.

(38) Griffith, O. W. Biologic and pharmacologic regulation of mammalian glutathione synthesis. *Free Radic.Biol. Med.* **1999**, *27*, 922-935.

(39) Briones-Herrera, A.; Eugenio-Perez, D.; Reyes-Ocampo, J. G.; Rivera-Mancia, S.; Pedraza-Chaverri, J. New highlights on the health-improving effects of sulforaphane. *Food Funct.* **2018**, *9*, 2589-2606.

(40) Houghton, C. A.; Fassett, R. G.; Coombes, J. S. Sulforaphane: translational research from laboratory bench to clinic. *Nutr. Rev.* **2013**, *71*, 709-726.

(41) Watanabe, M.; Fuda, H.; Okabe, H.; Joko, S.; Miura, Y.; Hui, S. P.; Yimin;

Hamaoka, N.; Miki, E.; Chiba, H. Oyster extracts attenuate pathological changes in non-alcoholic steatohepatitis (NASH) mouse model. *J. Funct. Foods* **2016**, *20*, 516-531.

(42) Masuda, S.; Kanamori, H.; Kinae, N. Isolation of mutagenic beta-carboline derivatives after nitrite treatment of maillard reaction mixtures and analysis of these compounds from foodstuffs and human urine. *Biosci. Biotechnol. Biochem.* **2005**, *69*, 2232-2235.

(43) Wang, M.; Jin, Y.; Li, J.; Ho, C. T. Two novel beta-carboline compounds from the Maillard reaction between xylose and tryptophan. *J. Agric. Food Chem.* **1999**, *47*, 48-50.

(44) Tamanna, N.; Mahmood, N. Food Processing and Maillard Reaction Products: Effect on Human Health and Nutrition. *Int. J. Food Sci.* **2015**, *2015*, 526762.

(45) Pyo, M. C.; Yang, S. Y.; Chun, S. H.; Oh, N. S.; Lee, K. W. Protective effects of Maillard reaction products of whey protein concentrate against oxidative stress through an Nrf2-dependent pathway in HepG2 cells. *Biol. Pharm. Bull.* **2016**, *39*, 1437-1447.

(46) Sauer, T.; Raithel, M.; Kressel, J.; Munch, G.; Pischetsrieder, M. Activation of the transcription factor Nrf2 in macrophages, Caco-2 cells and intact human gut tissue by Maillard reaction products and coffee. *Amino Acids* **2013**, *44*, 1427-1439.

(47) Mottram, D. S.; Wedzicha, B. L.; Dodson, A. T. Acrylamide is formed in the

Maillard reaction. *Nature* **2002**, *419*, 448-489.

(Figure captions)

Figure 1. Structures of flazin (**1**) perlolyrine (**2**), the flazin analogues (**3**-**6**) and the antioxidants (**7** & **8**) used in this study.

Figure 2. Synthetic route of perlolyrine (**2**) used in this study.

Figure 3. The structure-activity relationships of flazin, perlolyrine and flazin analogues were studied with reporter gene assays (A) and cytoprotection assays against AAPH (B). (A) Reporter gene assay for flazin (**1**), perlolyrine (**2**), flazin analogues (**3**-**6**), curcumin (**7**), and chlorogenic acid (**8**). The data are expressed as the fold increase in luciferase activity compared to that under control conditions (0 μM). (B) Cell viability in the presence of flazin (**1**), perlolyrine (**2**), flazin analogues (**3**-**6**), curcumin (**7**), and chlorogenic acid (**8**). The cells were incubated with 0 mM (-) or 15 mM (+) compound for 24 h. The data are expressed as the viability percentage relative to that under control conditions (0 μM). *$p < 0.05$, **$p < 0.01$, ***$p < 0.001$, ns: not significant (one-way ANOVA) (n = 6).

Figure 4. Nuclear translocation of Nrf2, and expression of Nrf2 and Keap1 by

flazin (**1**) in C3A cells. (A) Nuclear Nrf2 levels. Also shown is a Western blot of the relative Nrf2 levels in which lamin B1 was used as the internal control. (B) Cytoplasmic Nrf2 levels. Also shown is a Western blot of the relative Nrf2 levels in which GAPDH (glyceraldehyde-3-phosphate dehydrogenase) was as internal control. (C) Nrf2 levels in total lysates. Also shown is a Western blot of the relative Nrf2 levels in which GAPDH was as internal control. (D) Gene expression levels of Nrf2 as determined by real-time PCR analysis. The level of GAPDH expression was used as an internal control. (E) Keap1 levels in total lysates. Also shown is a Western blot of the relative Keap1 levels in which GAPDH was as internal control. The data are expressed as the fold increase in expression relative to the expression under control conditions (0 μM). *$p < 0.05$, **$p < 0.01$, ***$p < 0.001$, ns: not significant versus the control (one-way ANOVA) (n = 6).

Figure 5. Expression of Nrf2 target genes and proteins induced by flazin in C3A. (A) Relative expression of Nrf2 target genes as determined by real-time PCR analysis. The level of GAPDH expression was used as an internal control. The data are expressed as the fold increase in expression relative to the expression

under control conditions (0 μM). (B) Protein expression levels and a Western blot of the relative expression levels of NAD(P)H: quinine oxidoreductase 1 (NQO1) (n=6); GAPDH (glyceraldehyde-3-phosphate dehydrogenase) was used as the internal control. The protein expression and a Western blot showing the relative expression levels of glutathione S-transferase pi (GSTP) (n=6) are also shown; GAPDH was used as the internal control. The concentrations of glutathione (GSH) (n=6), which were normalized to the levels of total protein (n=6), are shown. *$p < 0.05$, **$p < 0.01$, ***$p < 0.001$, ns: not significant versus the control (one-way ANOVA) (n = 6).

CAT, catalase; GCL, glutamate-cysteine ligase; GCLC, glutamate-cysteine ligase catalytic subunit; GCLM, glutamate-cysteine ligase modulatory subunit; GSH, glutathione; GSS, glutathione synthetase; GSSG, oxidized glutathione; GSTM, glutathione S-transferase mu; GSTP, glutathione S-transferase pi; GSTT, glutathione S-transferase theta; GPx, glutathione peroxidase; GR, glutathione reductase; HO-1, haem oxygenase-1; NQO1, NAD(P)H: quinine oxidoreductase 1; SOD1, superoxide dismutase 1.

Figure 6. Schematic model of cytoprotection by flazin (**1**) *via* the Keap1-Nrf2

pathway. ARE, antioxidant response element; BVR, biliverdin reductase; CAT, catalase; Cys, cysteine; CO, carbon monoxide; CYP, cytochrome p450; GCL, glutamate-cysteine ligase; GCLC, glutamate-cysteine ligase catalytic subunit; GCLM, glutamate-cysteine ligase modulatory subunit; GSH, glutathione; GSS, glutathione synthetase; GSSG, oxidized glutathione; GST, glutathione S-transferase; GPx, glutathione peroxidase; GR, glutathione reductase; HO-1, haem oxygenase-1; Keap1, Kelch-like ECH-associated protein 1; NQO1, NAD(P)H: quinine oxidoreductase 1; Nrf2, nuclear factor erythroid 2-related factor 2; sMaf, small Maf; SOD1, superoxide dismutase 1; γGS, γ-glutamylcysteine.

Figure 7. Correlation between the cytoprotective effects and log *P* values of natural antioxidants. The cytoprotection was expressed in the relative cell viability to that for the control (0 μM antioxidants, 15 mM AAPH). The open triangles and the solid triangles indicate the direct antioxidants and the indirect antioxidants, respectively, which fit the correlation line. The closed circles (flazin, j [sulforaphane] and k [DHMBA]) indicate the indirect antioxidants that do not fit the correlation line. In the scatter plot shown, 4 divisions (I-IV) have been made

on the basis of cytoprotection (dividing line at 3-fold greater than control values) and log *P* (dividing line at 3). The letters represent the antioxidants, as follows: (a) cyanidin-3-O-glucoside, (b) chlorogenic acid, (c) gallic acid, (d) rosmarinic acid, (e) perlolyrine, (f) quercetin, (g) isoliquiritigenin, (h) curcumin, (i) lycopene, (j) sulforaphane, and (k) DHMBA.

(Fig. 1)

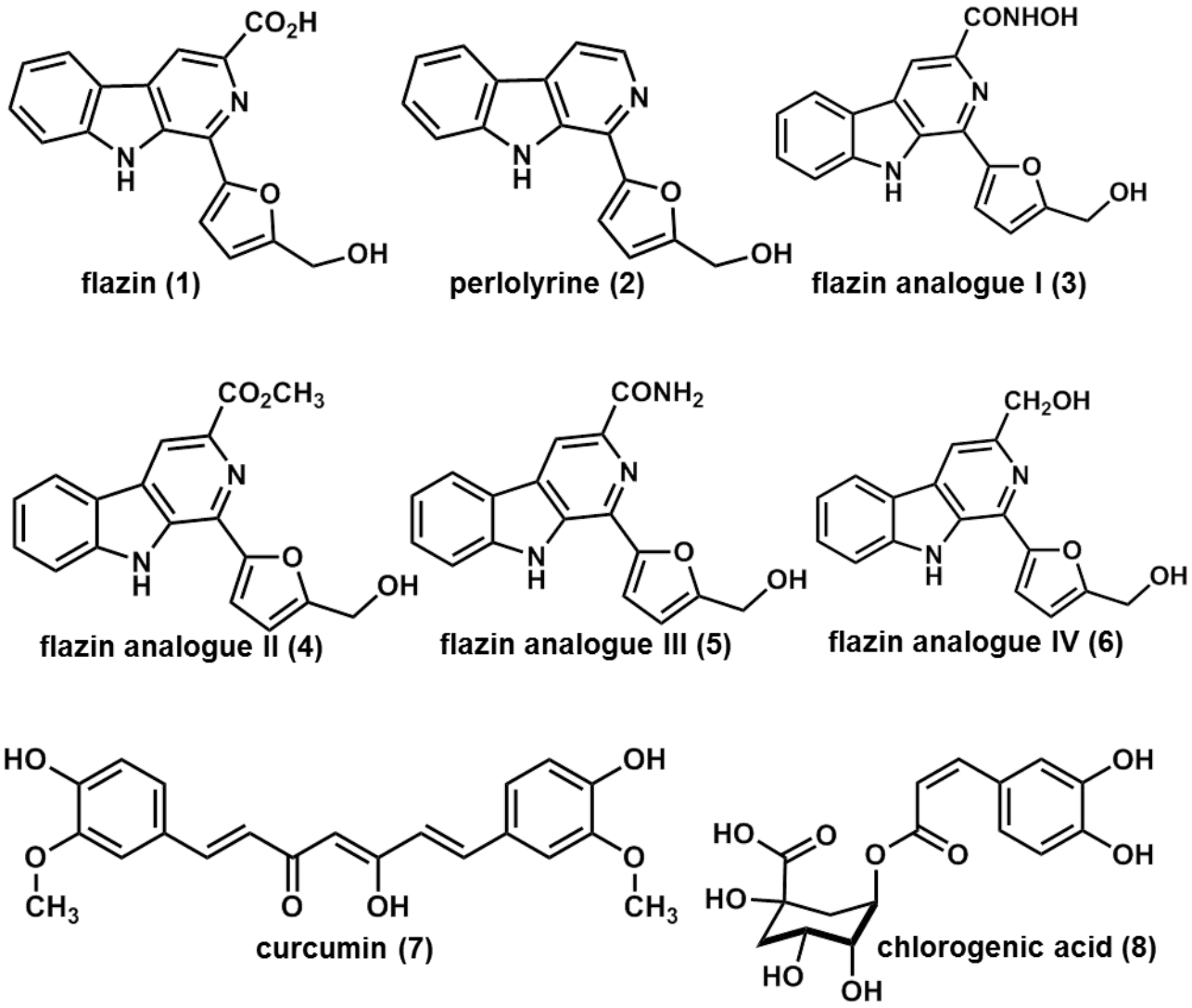

Figure 1. Structures of flazin (**1**) perlolyrine (**2**), the flazin analogues (**3**-**6**) and the antioxidants (**7** & **8**) used in this study.

(Fig. 2)

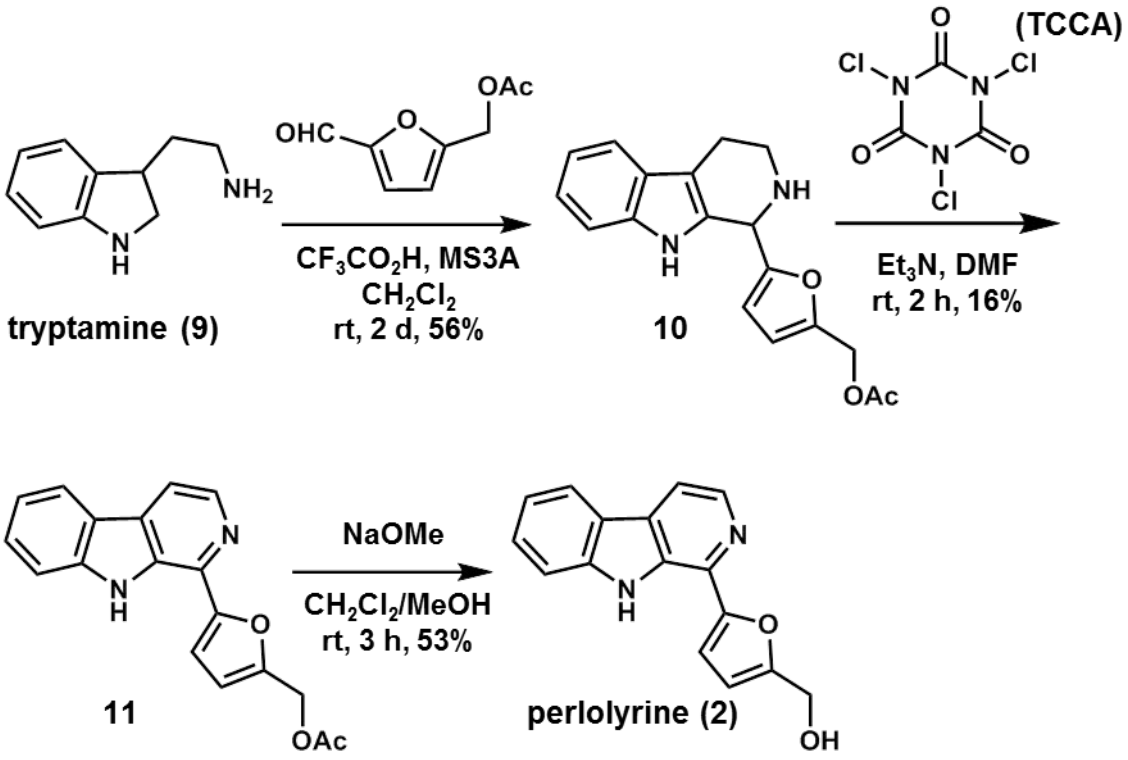

Figure 2. Synthetic route of perlolyrine (**2**) used in this study.

(Fig. 3)

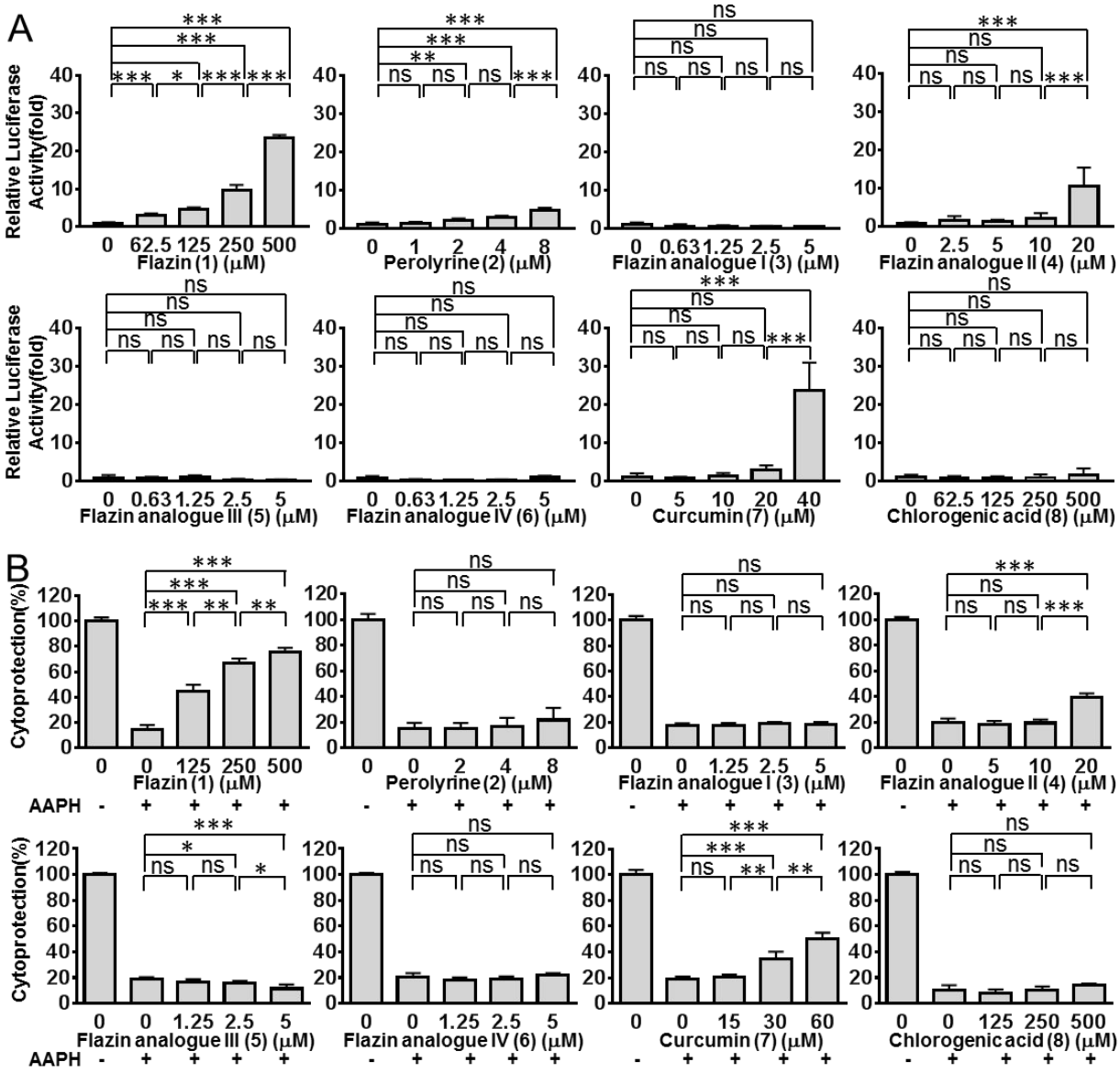

Figure 3. The structure-activity relationships of flazin, perlolyrine and flazin analogues were studied with reporter gene assays (A) and cytoprotection assays against AAPH (B). (A) Reporter gene assay for flazin (**1**), perlolyrine (**2**), flazin analogues (**3**-**6**), curcumin (**7**), and chlorogenic acid (**8**). The data are expressed as the fold increase in luciferase activity compared to that under control conditions (0 μM). (B) Cell viability in the presence of flazin (**1**), perlolyrine (**2**), flazin analogues (**3**-**6**), curcumin (**7**), and chlorogenic acid (**8**). The cells were incubated with 0 mM (-) or 15 mM (+) compound for 24 h. The data are expressed as the viability percentage relative to that under control conditions (0 μM). *p < 0.05, **p < 0.01, ***p < 0.001, ns: not

significant (one-way ANOVA) (n = 6).

(Fig. 4)

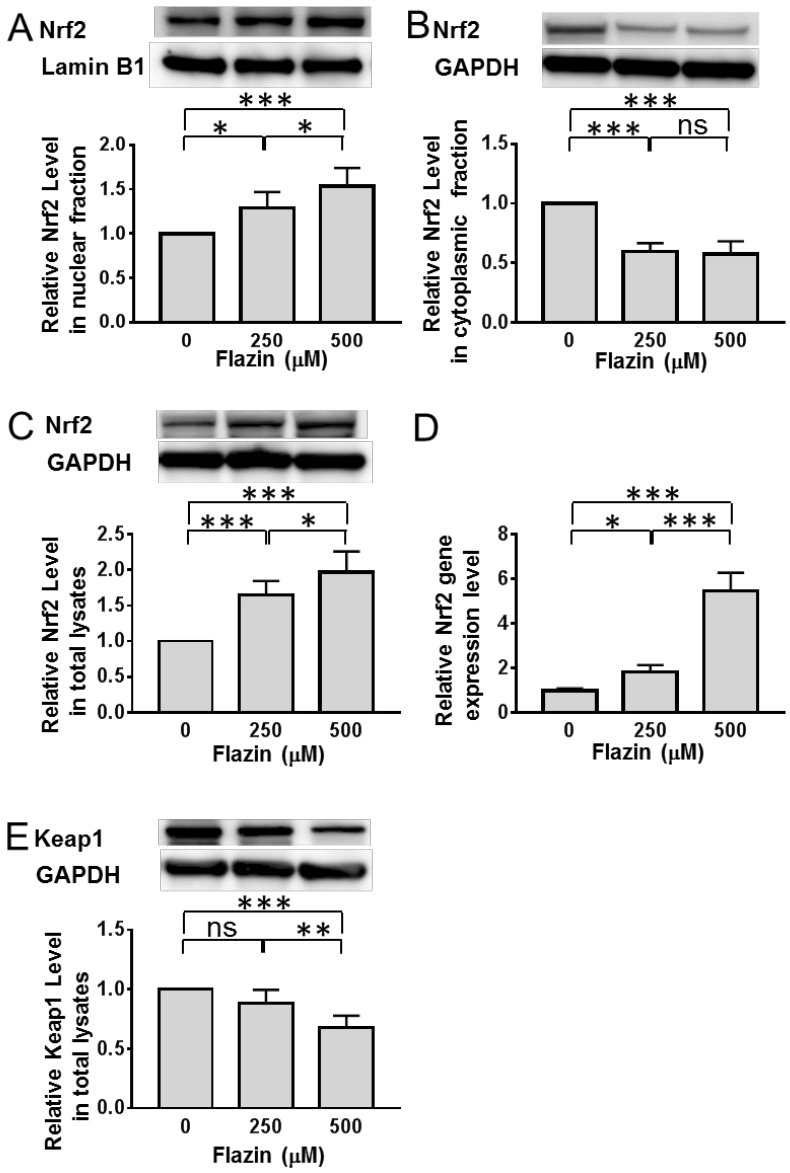

Figure 4. Nuclear translocation of Nrf2, and expression of Nrf2 and Keap1 by flazin (**1**) in C3A cells. (A) Nuclear Nrf2 levels. Also shown is a Western blot of the relative Nrf2 levels in which lamin B1 was used as the internal control. (B) Cytoplasmic Nrf2 levels. Also shown is a Western blot of the relative Nrf2 levels in which GAPDH (glyceraldehyde-3-phosphate dehydrogenase) was as internal control. (C) Nrf2 levels in total lysates. Also shown is a Western blot of the relative Nrf2 levels in which GAPDH was as internal control. (D) Gene expression levels of Nrf2 as determined by real-time PCR analysis. The level of GAPDH expression was used as an

internal control. (E) Keap1 levels in total lysates. Also shown is a Western blot of the relative Keap1 levels in which GAPDH was as internal control. The data are expressed as the fold increase in expression relative to the expression under control conditions (0 μM). *$p < 0.05$, **$p < 0.01$, ***$p < 0.001$, ns: not significant versus the control (one-way ANOVA) (n = 6).

(Fig. 5)

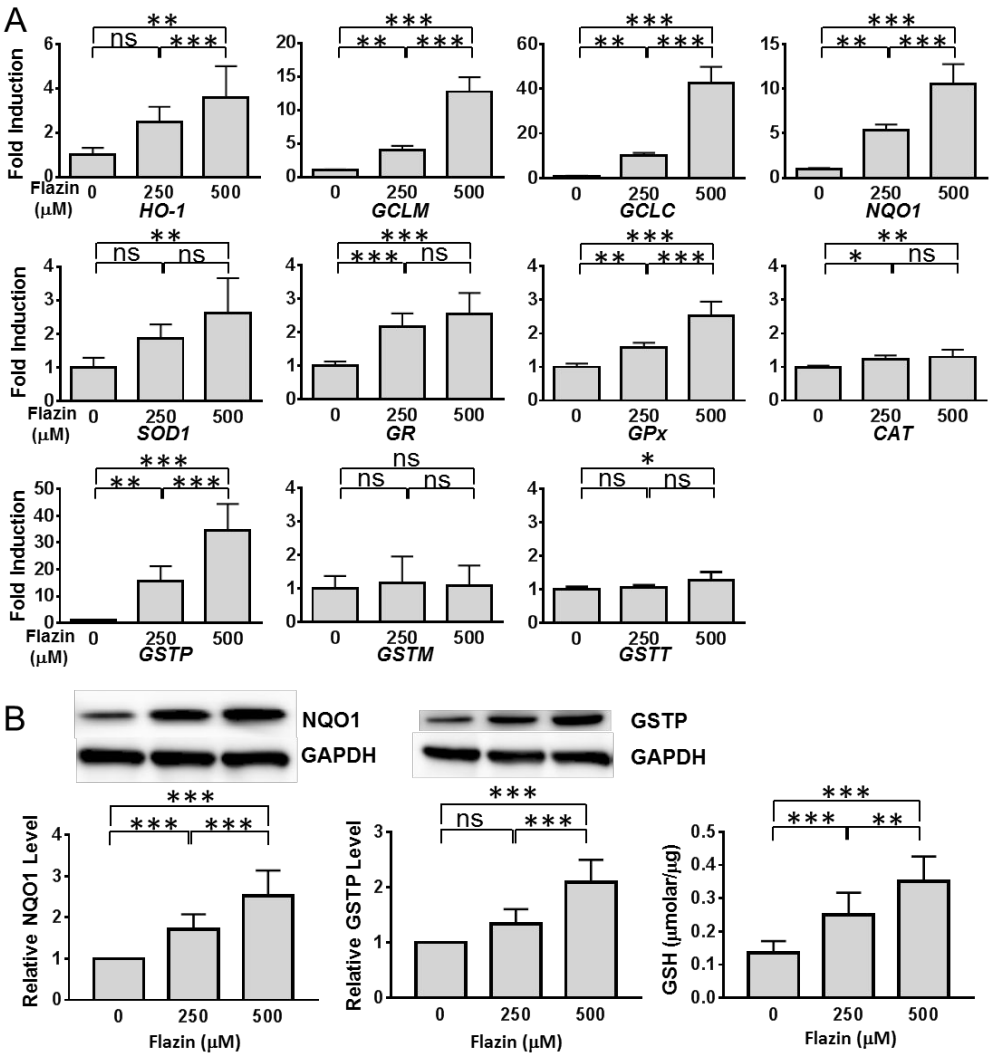

Figure 5. Expression of Nrf2 target genes and proteins induced by flazin in C3A. (A) Relative expression of Nrf2 target genes as determined by real-time PCR analysis. The level of GAPDH expression was used as an internal control. The data are expressed as the fold increase in expression relative to the expression under control conditions (0 μM). (B) Protein expression levels and a Western blot of the relative expression levels of NAD(P)H: quinine oxidoreductase 1 (NQO1) (n=6); GAPDH (glyceraldehyde-3-phosphate dehydrogenase) was used as the internal control. The protein expression and a Western blot showing the relative expression levels of glutathione S-transferase pi (GSTP) (n=6) are also shown; GAPDH was used as the internal

control. The concentrations of glutathione (GSH) (n=6), which were normalized to the levels of total protein (n=6), are shown. *p < 0.05, **p < 0.01, ***p < 0.001, ns: not significant versus the control (one-way ANOVA) (n = 6). CAT, catalase; GCL, glutamate-cysteine ligase; GCLC, glutamate-cysteine ligase catalytic subunit; GCLM, glutamate-cysteine ligase modulatory subunit; GSH, glutathione; GSS, glutathione synthetase; GSSG, oxidized glutathione; GSTM, glutathione S-transferase mu; GSTP, glutathione S-transferase pi; GSTT, glutathione S-transferase theta; GPx, glutathione peroxidase; GR, glutathione reductase; HO-1, haem oxygenase-1; NQO1, NAD(P)H: quinine oxidoreductase 1; SOD1, superoxide dismutase 1.

(Fig. 6)

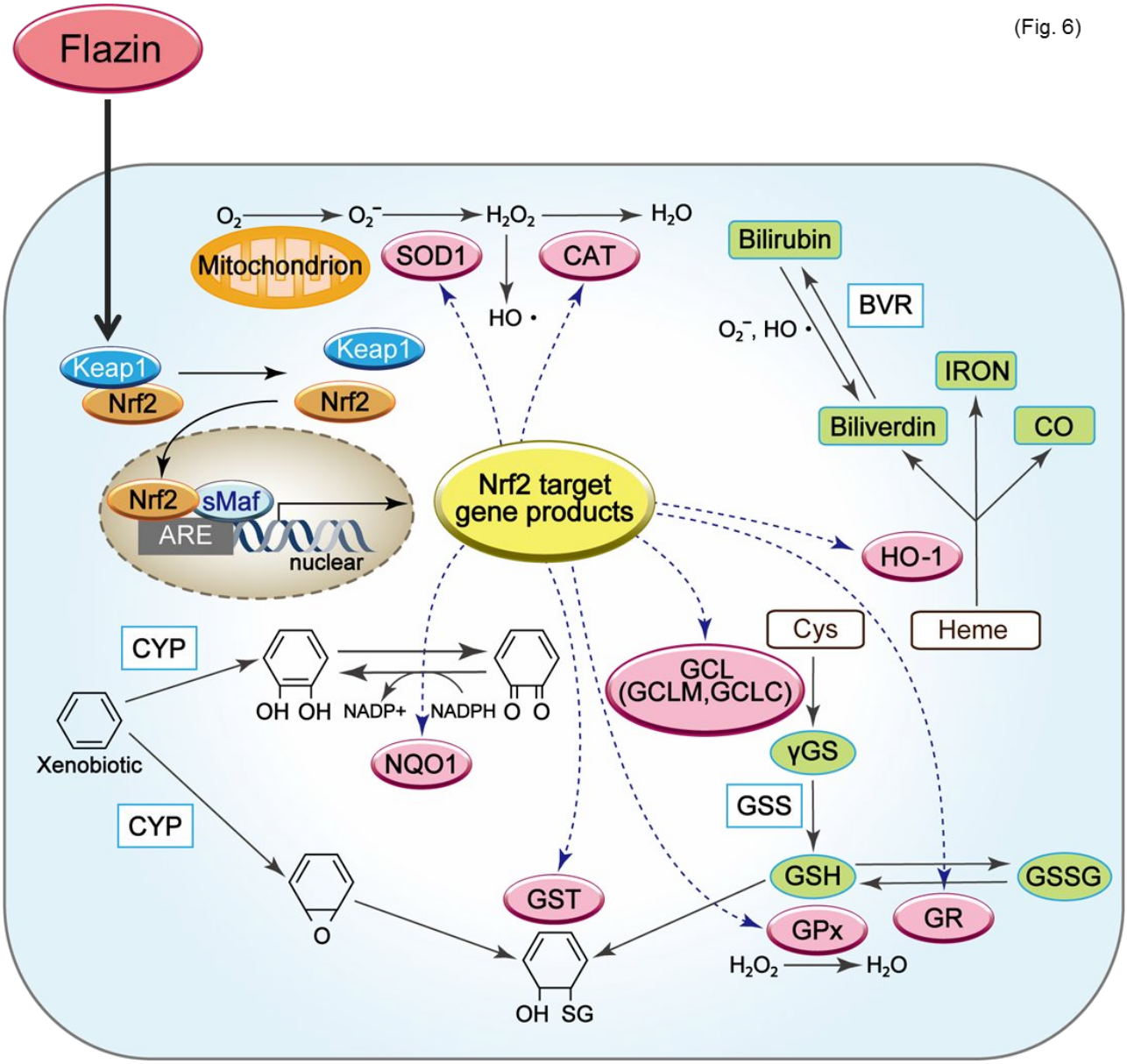

Figure 6. Schematic model of cytoprotection by flazin (**1**) *via* the Keap1-Nrf2 pathway. ARE, antioxidant response element; BVR, biliverdin reductase; CAT, catalase; Cys, cysteine; CO, carbon monoxide; CYP, cytochrome p450; GCL, glutamate-cysteine ligase; GCLC, glutamate-cysteine ligase catalytic subunit; GCLM, glutamate-cysteine ligase modulatory subunit; GSH, glutathione; GSS, glutathione synthetase; GSSG, oxidized glutathione; GST, glutathione S-transferase; GPx, glutathione peroxidase; GR, glutathione reductase; HO-1, haem oxygenase-1; Keap1, Kelch-like ECH-associated protein 1; NQO1, NAD(P)H: quinine oxidoreductase 1; Nrf2, nuclear factor erythroid 2-related factor 2; sMaf, small Maf; SOD1, superoxide dismutase 1; γGS, γ-glutamylcysteine.

(Fig. 7)

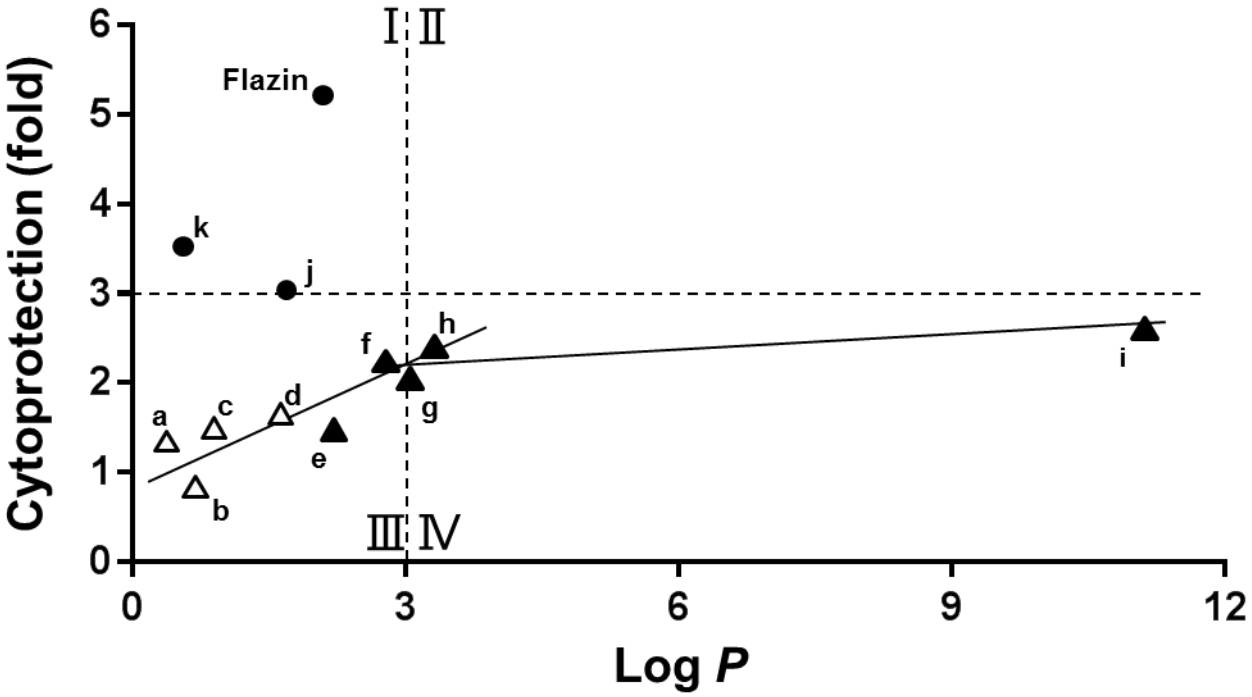

Figure 7. Correlation between the cytoprotective effects and log *P* values of natural antioxidants. The cytoprotection was expressed in the relative cell viability to that for the control (0 μM antioxidants, 15 mM AAPH). The open triangles and the solid triangles indicate the direct antioxidants and the indirect antioxidants, respectively, which fit the correlation line. The closed circles (flazin, j [sulforaphane] and k [DHMBA]) indicate the indirect antioxidants that do not fit the

correlation line. In the scatter plot shown, 4 divisions (I-IV) have been made on the basis of cytoprotection (dividing line at 3-fold greater than control values) and log *P* (dividing line at 3). The letters represent the antioxidants, as follows: (a) cyanidin-3-O-glucoside, (b) chlorogenic acid, (c) gallic acid, (d) rosmarinic acid, (e) perlolyrine, (f) quercetin, (g) isoliquiritigenin, (h) curcumin, (i) lycopene, (j) sulforaphane, and (k) DHMBA.

Table 1. Summarized characteristics of studied antioxidants.

Compounds	IC_{50} (μM)	Relative ORAC value (μmol of TE/μmol)	Keap1-Nrf2 activity (fold)	Cytoprotection (fold)	*n*-Octanol/water partition coefficient (log *P*)	References
Flazin (**1**)	500<	1.43 ± 0.11 2	23.4 ± 0.861	5.21 ± 0.245	2.1[a]	this study
Perlolyrin (**2**)	11.0	1.60 ± 0.230	4.64 ± 0.812	1.41 ± 0.607	2.2[a]	this study
Flazin analogue I (**3**)	51.5	3.65 ± 0.392	0.45 3± 0.263	1.01 ± 0.123	1.72[b]	this study
Flazin analogue II (**4**)	88.2	0.587± 0.124	10.5 ± 4.95	2.00 ± 0.176	2.80[b]	this study
Flazin analogue III (**5**)	12.0	0.886± 0.0735	0.332 ± 0.216	0.873 ± 0.103	2.01[b]	this study
Flazin analogue IV (**6**)	24.4	2.50 ± 0.287	1.00 ± 0.480	1.06 ± 0.0809	2.45[b]	this study
Cyanidin-3-O-glucoside	500 <	1.06± 0.0412	0.810± 0.124	1.29± 0.110	0.39[c]	Joko et al. (2017). Journal of Functional Foods, 35, 245-255.
Chlorogenic acid (**8**)	500 <	4.57± 0.303	0.912± 0.203	0.774± 0.320	0.69[d]	Watanabe et al. (2012). Journal of Agricultural Food Chemistry, 60, 830-835; Fuda et al. (2015). Food Chemistry, 176, 226-233; Joko et al. (2017). Journal of Functional Foods, 35, 245-255.
Gallic acid	400 <	1.47± 0.121	0.901± 0.330	1.42± 0.219	0.91[d]	Joko et al. (2017). Journal of Functional Foods, 35, 245-255.
Rosmarinic acid	400 <	11.5± 0.562	1.13± 0.340	1.61± 0.268	1.6[e]	Joko et al. (2017). Journal of Functional Foods, 35, 245-255.
DHMBA	500 <	1.47± 0.401	5.58± 0.634	3.50± 0.31 2	0.561± 0.190[f]	Watanabe et al. (2012). Journal of Agricultural Food Chemistry, 60, 830-835; Fuda et al. (2015). Food Chemistry, 176, 226-233; Joko et al. (2017). Journal of Functional Foods, 35, 245-255.
Sulforaphane	296	n.d.	15.4± 4.75	2.97± 0.166	1.68[g]	Joko et al. (2017). Journal of Functional Foods, 35, 245-255.
Quercetin	199	1.57± 0.303	12.8± 1.11	2.15± 0.0312	2.74[h]	Joko et al. (2017). Journal of Functional Foods, 35, 245-255.
Isoliquiritigenin	153	6.50± 0.332	40.1± 9.41	2.00± 0.161	3.04[i]	Joko et al. (2017). Journal of Functional Foods, 35, 245-255.
Curcumin (**7**)	109	8.12± 0.831	23.8 ± 7.30	2.66± 0.253	3.29[j]	Joko et al. (2017). Journal of Functional Foods, 35, 245-255.
Lycopene	110	n.d.	18.7± 1.03	2.63± 0.248	11.11[k]	Joko et al. (2017). Journal of Functional Foods, 35, 245-255.

Keap1-Nrf2 activity was expressed in the relative activity to that for the control (0 μM). The cytoprotection was expressed in the relative cell viability to that for the control (0 □M antioxidants, 15 mM AAPH). The values of cell cytotoxicity (IC_{50}) were determined by non-linear transform. Each value was expressed in average ± SD. n.d.: not detected. [a] PubChem. https://pubchem.ncbi.nlm.nih.gov/ [b] Virtual Computational Chemistry Laboratory. http://www.vcclab.org/ [c] Olivas-Aguirre et al. (2016). Molecules, 21, 1264. [d] Sergediene et al. (1999). FEBS Letter. 462, 392-396. [e] Zhu et al. Bioscience, Biotechnology, and Biochemistry. 79, 1178-1182 (2015). [f] Joko *et al.* (2017). Journal of Functional Foods, 35, 245-255. [g] Avdeef & Tam. (2010). Journal of Medicinal Chemistry, 53, 3566-3584. [h] Sergediene *et al.* (1999). FEBS Letter, *462*, 392-396. [i] Tanemoto et al. (2015). Biochemistry and Biophysics Reports, *2*, 153-159. [j] Ramalingam, Yoo, and Ko. (2016). Food Research International, 84, 113-119. [k] Goupy, Reynaud, Dangles, and Caris-Veyrat. (2012). New Journal of Chemistry, 36, 575-587.

(Abstract graphic)

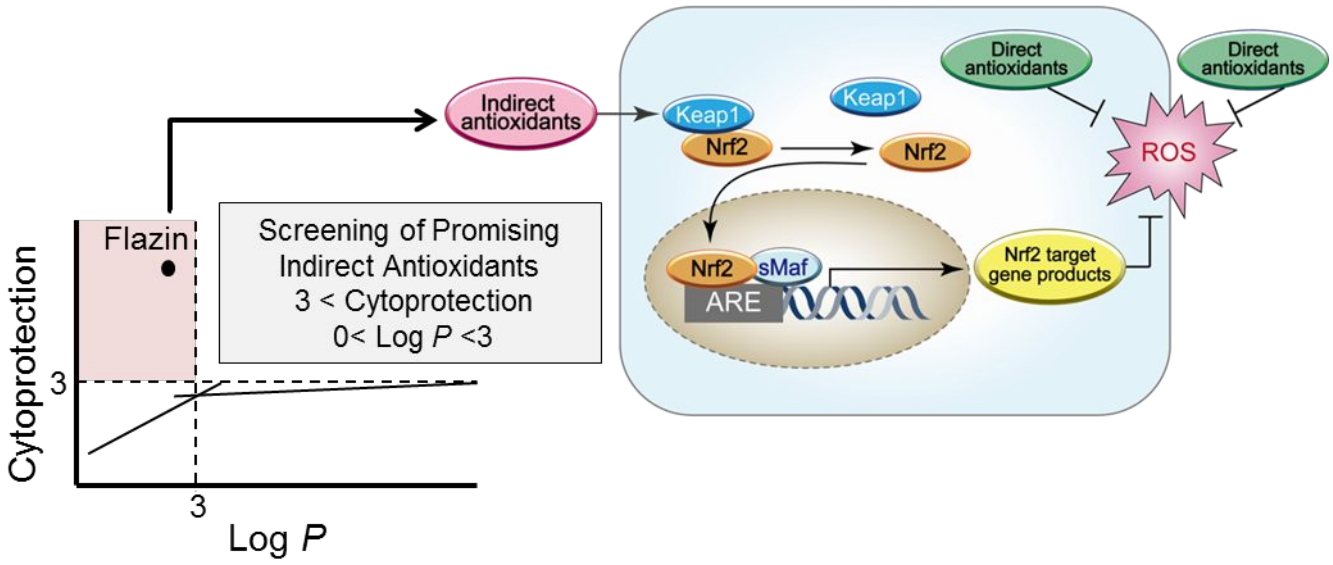

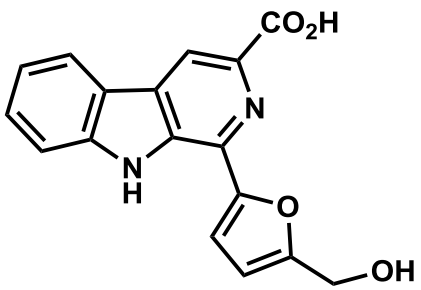

flazin (1)

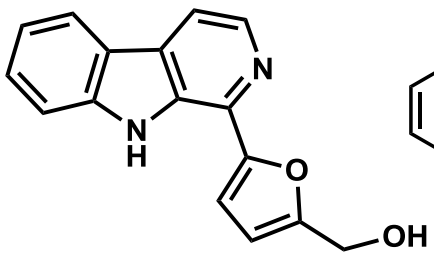

perlolyrine (2)

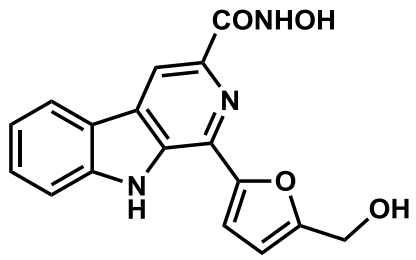

flazin analogue I (3)

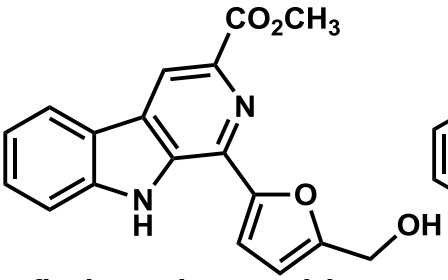

flazin analogue II (4)

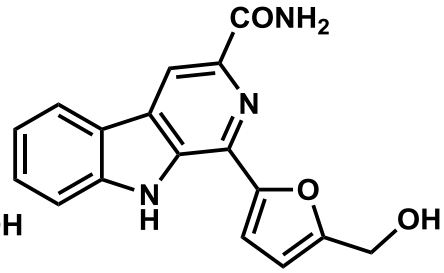

flazin analogue III (5)

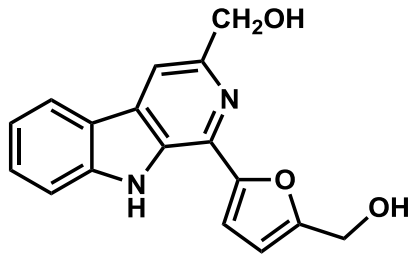

flazin analogue IV (6)

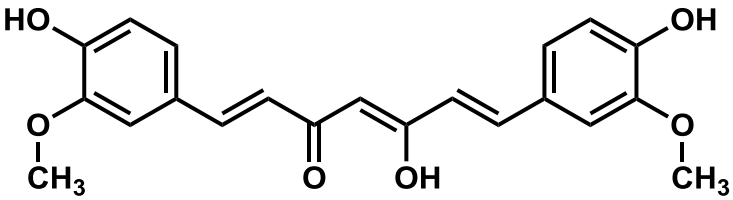

curcumin (7)

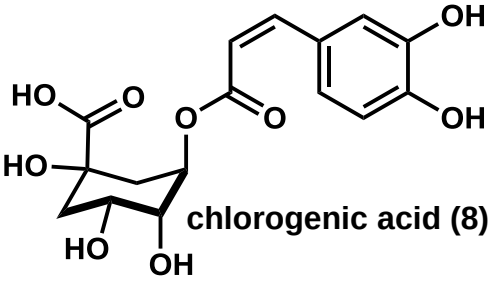

chlorogenic acid (8)

(Fig. 2)

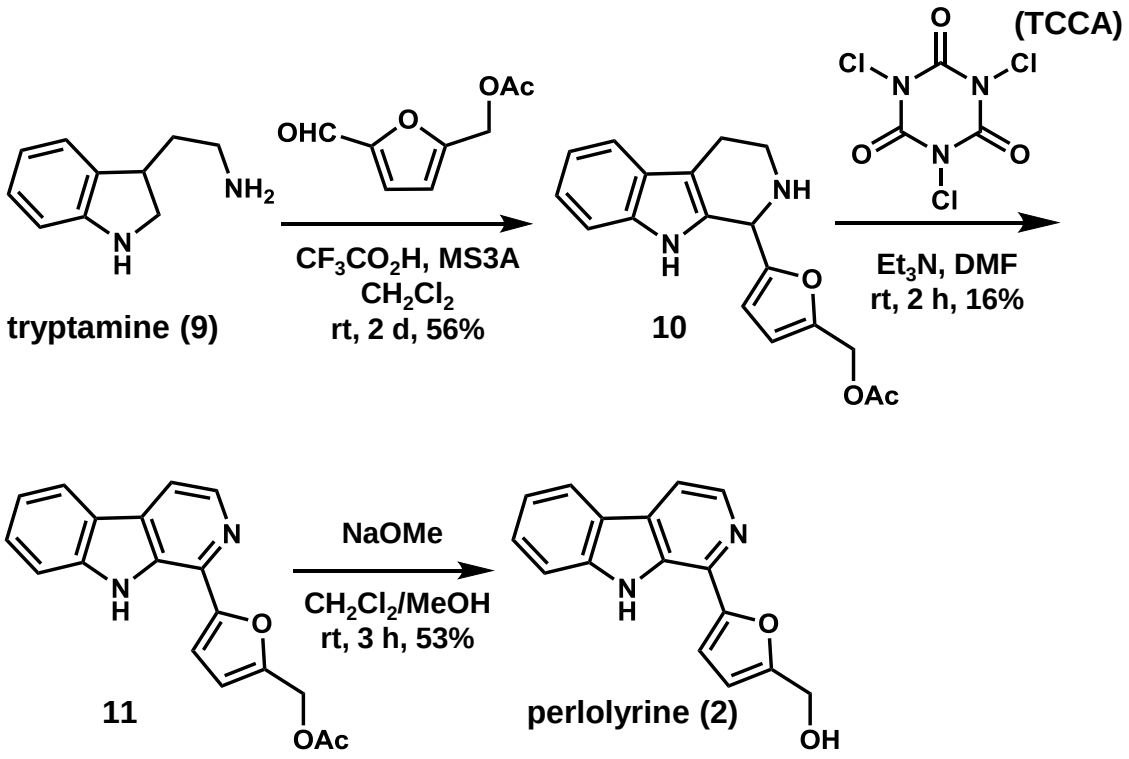
(TCCA)
tryptamine (9)
CF_3CO_2H, MS3A
CH_2Cl_2
rt, 2 d, 56%
10
Et_3N, DMF
rt, 2 h, 16%
11
NaOMe
CH_2Cl_2/MeOH
rt, 3 h, 53%
perlolyrine (2)

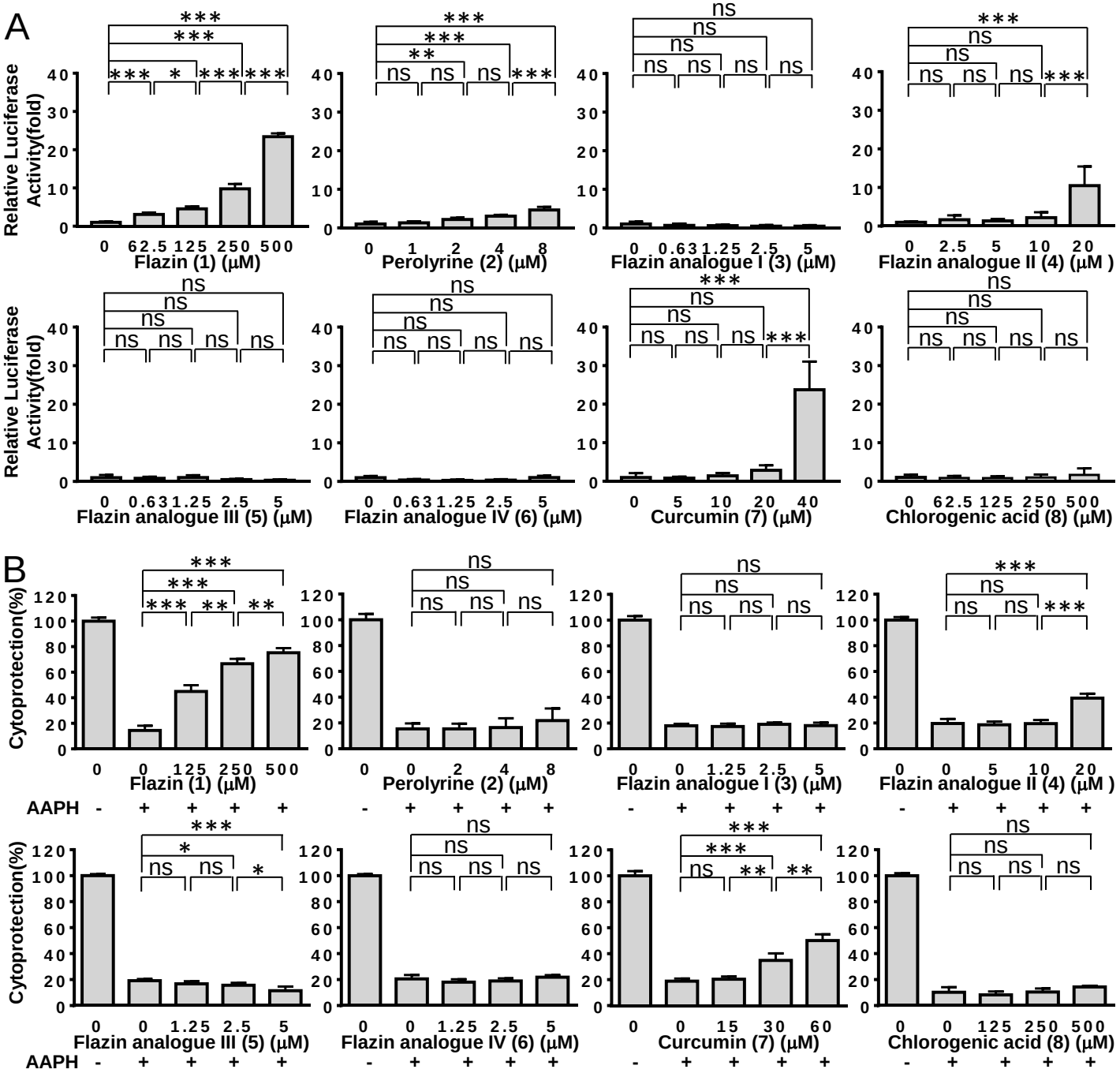
A
Relative Luciferase Activity(fold)
Flazin (1) (μM)
Perolyrine (2) (μM)
Flazin analogue I (3) (μM)
Flazin analogue II (4) (μM)
Flazin analogue III (5) (μM)
Flazin analogue IV (6) (μM)
Curcumin (7) (μM)
Chlorogenic acid (8) (μM)
B
Cytoprotection(%)
AAPH

(Fig. 4)

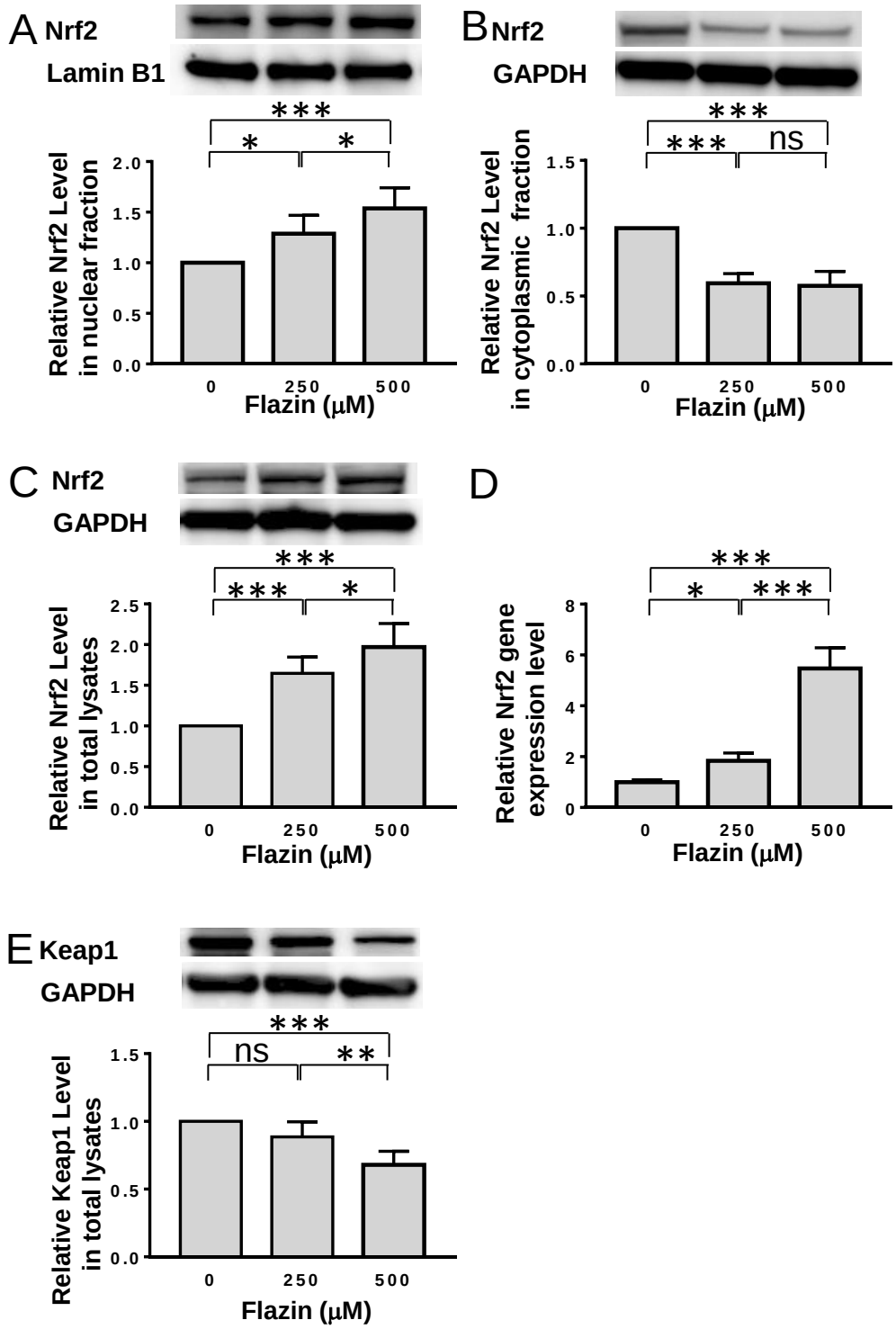
A
Nrf2
Lamin B1
***
*
*
Relative Nrf2 Level in nuclear fraction
2.0
1.5
1.0
0.5
0.0
0
250
500
Flazin (μM)
B
Nrf2
GAPDH
***
***
ns
Relative Nrf2 Level in cytoplasmic fraction
1.5
1.0
0.5
0.0
0
250
500
Flazin (μM)
C
Nrf2
GAPDH
***
***
*
Relative Nrf2 Level in total lysates
2.5
2.0
1.5
1.0
0.5
0.0
0
250
500
Flazin (μM)
D
***
*
***
Relative Nrf2 gene expression level
8
6
4
2
0
0
250
500
Flazin (μM)
E
Keap1
GAPDH
***
ns
**
Relative Keap1 Level in total lysates
1.5
1.0
0.5
0.0
0
250
500
Flazin (μM)

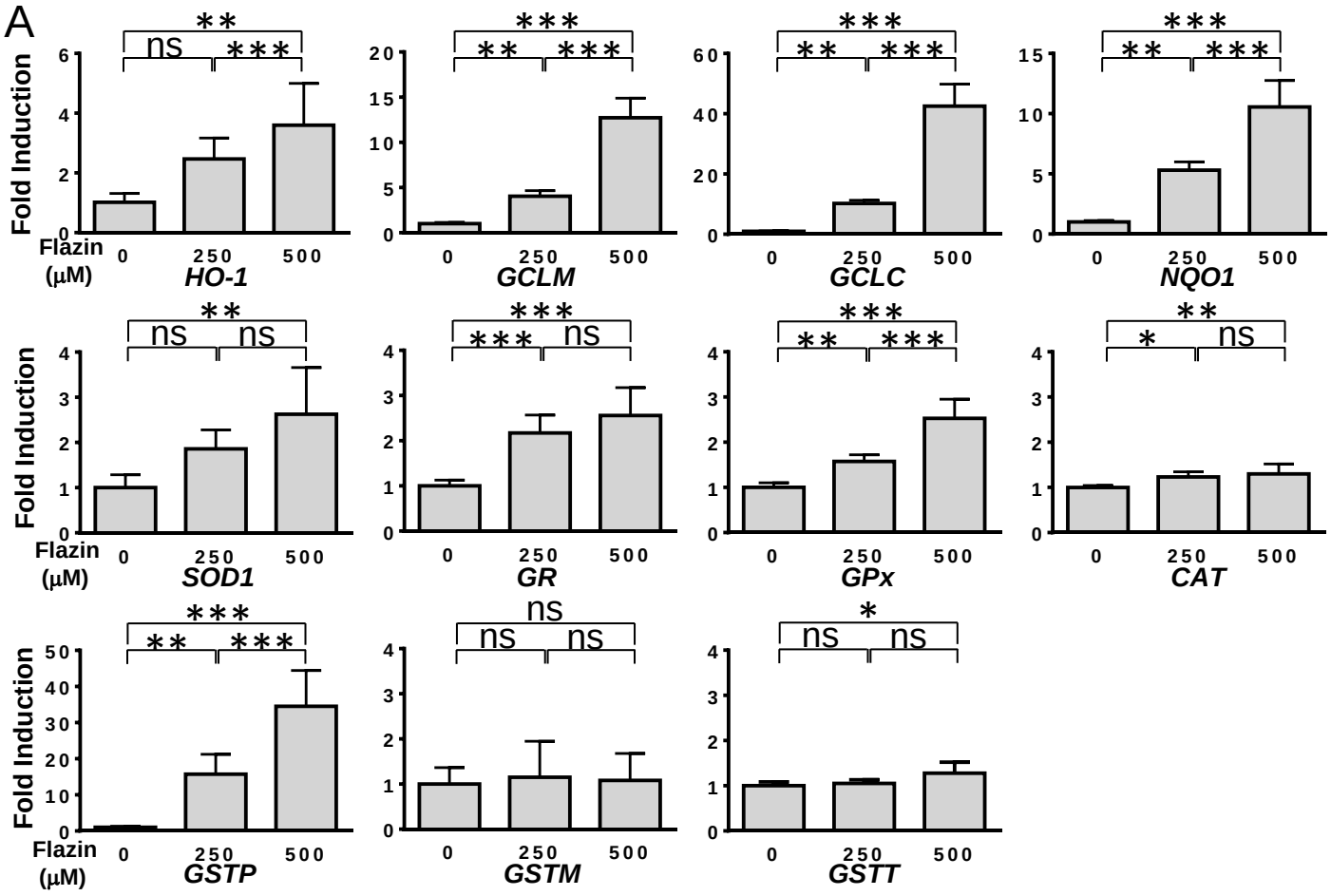
A
Fold Induction
Flazin (μM)
0
250
500
HO-1
GCLM
GCLC
NQO1
SOD1
GR
GPx
CAT
GSTP
GSTM
GSTT
ns
*
**
***

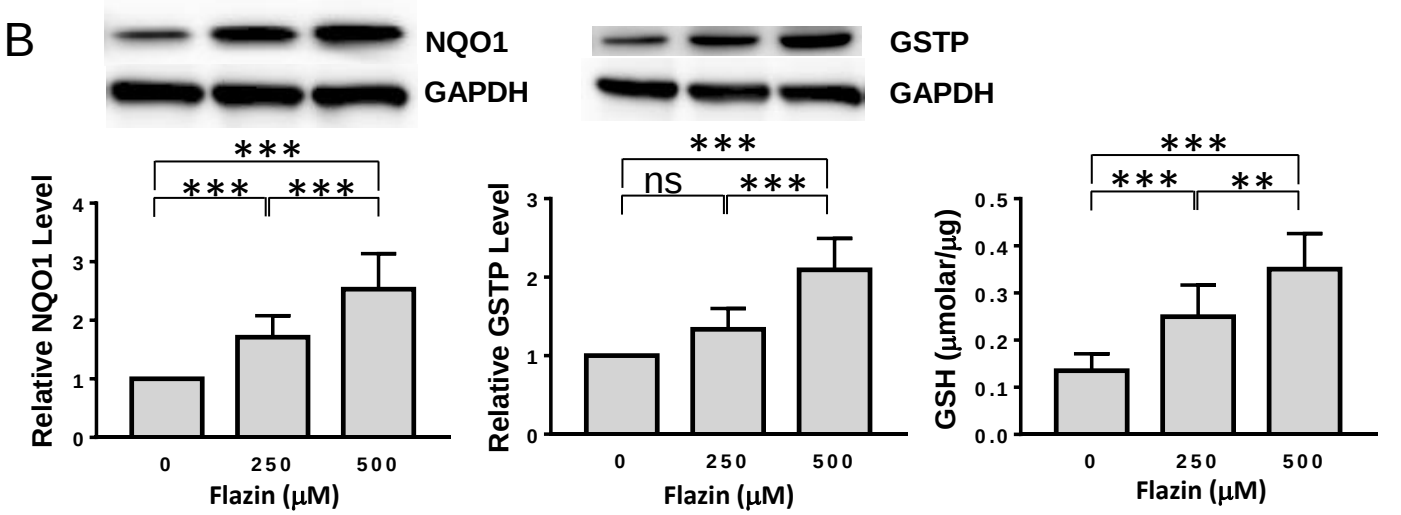
B
NQO1
GAPDH
GSTP
GAPDH
Relative NQO1 Level
Relative GSTP Level
GSH (μmolar/μg)
Flazin (μM)
0
250
500
ns
***
**

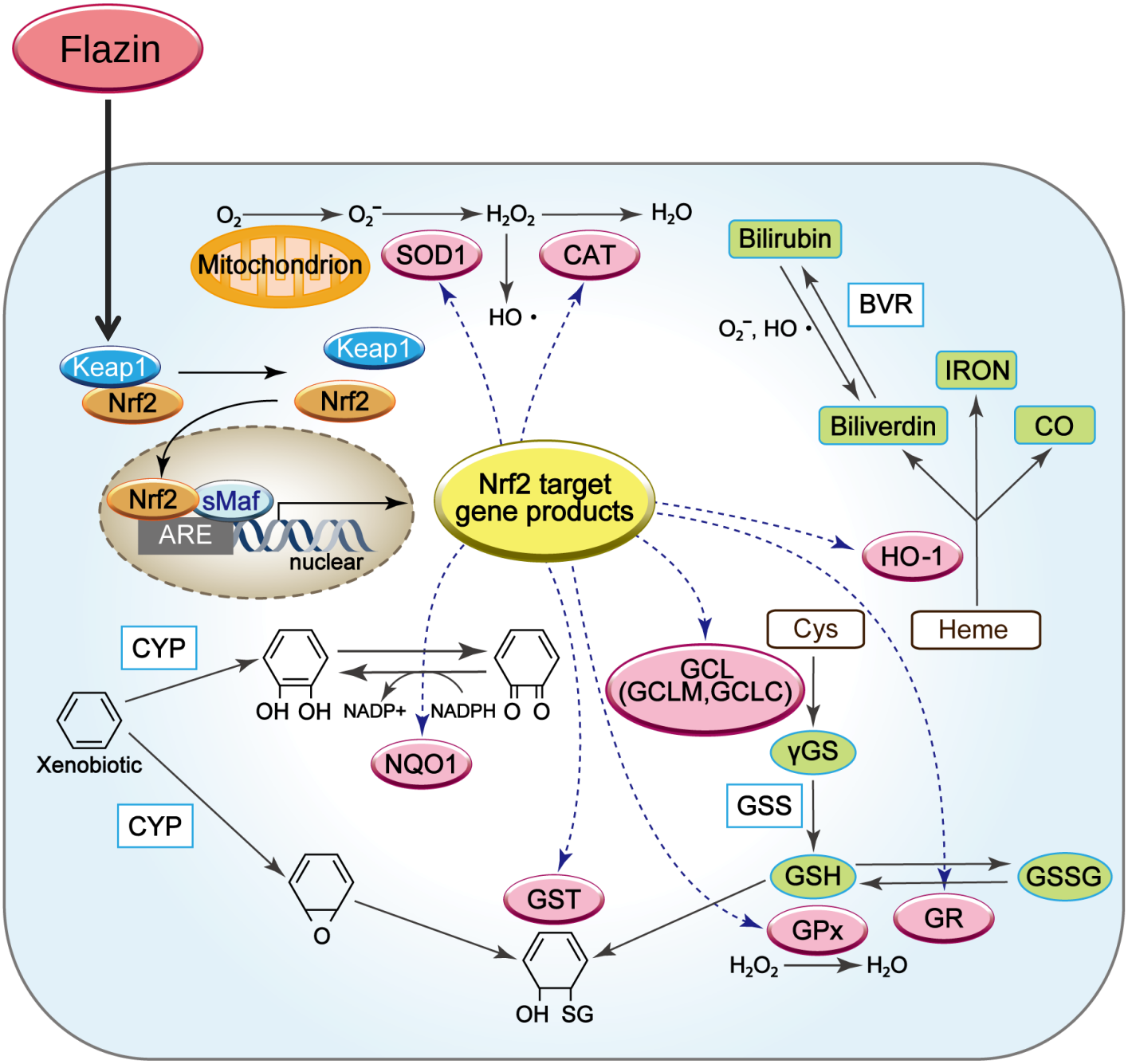
Flazin
O_2
O_2^-
H_2O_2
H_2O
Mitochondrion
SOD1
CAT
HO •
Bilirubin
BVR
O_2^-, HO •
IRON
Biliverdin
CO
Keap1
Nrf2
Keap1
Nrf2
Nrf2
sMaf
ARE
nuclear
Nrf2 target gene products
HO-1
Cys
Heme
CYP
OH OH
NADP+
NADPH
O O
GCL (GCLM,GCLC)
Xenobiotic
NQO1
γGS
GSS
CYP
GSH
GSSG
GST
GR
GPx
O
H_2O_2
H_2O
OH SG

(Fig. 7)

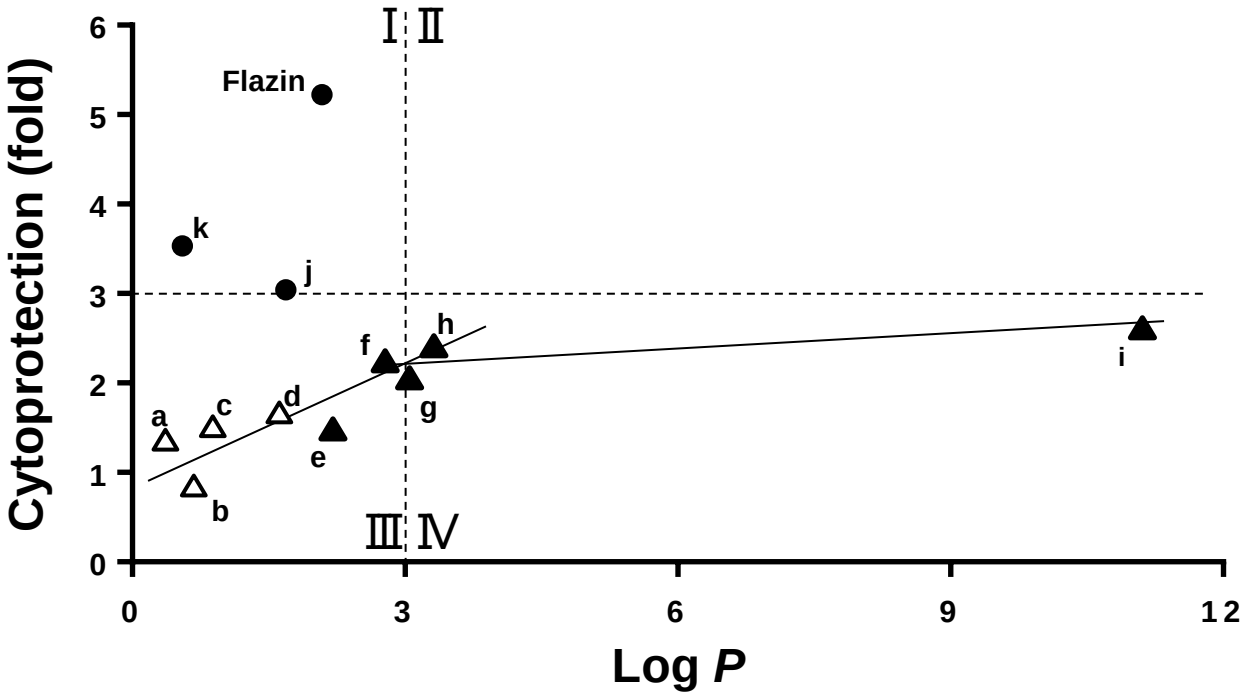
Cytoprotection (fold)
Log P
Ⅰ
Ⅱ
Ⅲ
Ⅳ
Flazin
a
b
c
d
e
f
g
h
i
j
k
0
1
2
3
4
5
6
0
3
6
9
12

(Table 1)

Table 1. Summarized characteristics of studied antioxidants.

Compounds	IC_{50} (μM)	Relative ORAC value (μmol of TE/μmol)	Keap1-Nrf2 activity (fold)	Cytoprotection (fold)	*n*-Octanol/water partition coefficient (log *P)*	References
Flazin (**1**)	500<	1.43 ± 0.11 2	23.4 ± 0.861	5.21 ± 0.245	2.1[a]	this study
Perlolyrin (**2**)	11.0	1.60 ± 0.230	4.64 ± 0.812	1.41 ± 0.607	2.2[a]	this study
Flazin analogue I (**3**)	51.5	3.65 ± 0.392	0.45 3± 0.263	1.01 ± 0.123	1.72[b]	this study
Flazin analogue II (**4**)	88.2	0.587± 0.124	10.5 ± 4.95	2.00 ± 0.176	2.80[b]	this study
Flazin analogue III (**5**)	12.0	0.886± 0.0735	0.332 ± 0.216	0.873 ± 0.103	2.01[b]	this study
Flazin analogue IV (**6**)	24.4	2.50 ± 0.287	1.00 ± 0.480	1.06 ± 0.0809	2.45[b]	this study
Cyanidin-3-O-glucoside	500 <	1.06±0.0412	0.810±0.124	1.29±0.110	0.39[c]	Joko et al. (2017). Journal of Functional Foods, 35, 245-255.
Chlorogenic acid (**8**)	500 <	4.57±0.303	0.912±0.203	0.774±0.320	0.69[d]	Watanabe et al. (2012). Journal of Agricultural Food Chemistry, 60, 830-835; Fuda et al. (2015). Food Chemistry, 176, 226-233; Joko et al. (2017). Journal of Functional Foods, 35, 245-255.
Gallic acid	400 <	1.47±0.121	0.901±0.330	1.42±0.219	0.91[d]	Joko et al. (2017). Journal of Functional Foods, 35, 245-255.
Rosmarinic acid	400 <	11.5±0.562	1.13±0.340	1.61±0.268	1.6[e]	Joko et al. (2017). Journal of Functional Foods, 35, 245-255.
DHMBA	500 <	1.47±0.401	5.58±0.634	3.50±0.31 2	0.561±0.190[f]	Watanabe et al. (2012). Journal of Agricultural Food Chemistry, 60, 830-835; Fuda et al. (2015). Food Chemistry, 176, 226-233; Joko et al. (2017). Journal of Functional Foods, 35, 245-255.
Sulforaphane	296	n.d.	15.4±4.75	2.97±0.166	1.68[g]	Joko et al. (2017). Journal of Functional Foods, 35, 245-255.
Quercetin	199	1.57±0.303	12.8±1.11	2.15±0.0312	2.74[h]	Joko et al. (2017). Journal of Functional Foods, 35, 245-255.
Isoliquiritigenin	153	6.50±0.332	40.1±9.41	2.00±0.161	3.04[i]	Joko et al. (2017). Journal of Functional Foods, 35, 245-255.
Curcumin (**7**)	109	8.12±0.831	23.8 ±7.30	2.66±0.253	3.29[j]	Joko et al. (2017). Journal of Functional Foods, 35, 245-255.
Lycopene	110	n.d.	18.7±1.03	2.63±0.248	11.11[k]	Joko et al. (2017). Journal of Functional Foods, 35, 245-255.

Keap1-Nrf2 activity was expressed in the relative activity to that for the control (0 μM). The cytoprotection was expressed in the relative cell viability to that for the control (0 μM antioxidants, 15 mM AAPH). The values of cell cytotoxicity (IC_{50}) were determined by non-linear transform. Each value was expressed in average ± SD. n.d.: not detected. [a] PubChem. https://pubchem.ncbi.nlm.nih.gov/ [b] Virtual Computational Chemistry Laboratory. http://www.vcclab.org/ [c] Olivas-Aguirre et al. (2016). Molecules, 21, 1264. [d] Sergediene et al. (1999). FEBS Letter. 462, 392-396. [e] Zhu et al. Bioscience, Biotechnology, and Biochemistry. 79, 1178-1182 (2015). [f] Joko et al. (2017). Journal of Functional Foods, 35, 245-255. [g] Avdeef & Tam. (2010). Journal of Medicinal Chemistry, 53, 3566-3584. [h] Sergediene et al. (1999). FEBS Letter, *462*, 392-396. [i] Tanemoto et al. (2015). Biochemistry and Biophysics Reports, *2*, 153-159. [j] Ramalingam, Yoo, and Ko. (2016). Food Research International, 84, 113-119. [k] Goupy, Reynaud, Dangles, and Caris-Veyrat. (2012). New Journal of Chemistry, 36, 575-587.

(Abstract graphic)